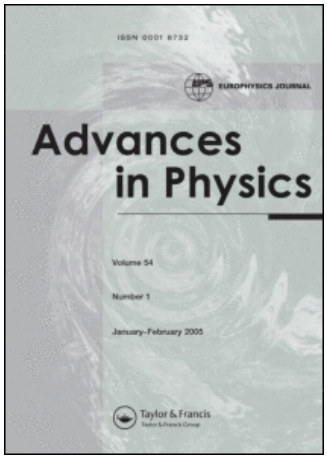

Advances in Physics
Publication details, including instructions for authors and subscription information:
http://www.informaworld.com/smpp/title~content=t713736250

Electron spin transitions in quantum Hall systems

Tapash Chakraborty

Online Publication Date: 01 December 2000
To cite this Article: Chakraborty, Tapash (2000) 'Electron spin transitions in quantum Hall systems', Advances in Physics, 49:8, 959 - 1014
To link to this article: DOI: 10.1080/00018730050198161
URL: http://dx.doi.org/10.1080/00018730050198161

ADVANCES IN PHYSICS, 2000, VOL. 49, NO. 8, 959–1014

Electron spin transitions in quantum Hall systems

TAPASH CHAKRABORTY†*
Max-Planck Institut für Physik Komplexer Systeme, D-01187 Dresden, Germany

[Received January 2000; revision received 20 June 2000; accepted 19 July 2000]

Abstract

A system of two-dimensional electron gas in a strong magnetic field exhibits a remarkable phenomenon known as the fractional quantum Hall effect. Rapid advances in experimental techniques and intense theoretical work for well over a decade have significantly contributed to our understanding of the mechanism behind the effect. It is now a well established fact that electron correlations are largely responsible for the occurrence of this phenomenon. In recent years, theoretical and experimental investigations have revealed that those electron correlations, which are responsible for the quantum Hall effect, are also the reason for various spin transitions in the system. In this review, we systematically follow the theoretical studies of the role spin degree of freedom play in the quantum Hall effect regime and also describe several ingenious experiments reported in recent years which are in good agreement with the emerging theoretical picture.

Contents PAGE

† Present address: Institute of Mathematical Sciences, Madras 600113, India.
* e-mail: tapash@mpipks-dresden.mpg.de

Advances in Physics ISSN 0001–8732 print/ISSN 1460–6976 online
http://www.tandf.co.uk /journals

1. Introduction

Discovery of the fractional quantum Hall effect (FQHE) in 1982 [1], only two years after the discovery of the integer quantum Hall effect (IQHE) [2] opened a new chapter in condensed matter physics which has, over all these years, enriched the field with a wide variety of interesting and often unexpected phenomena [3–6] related to electron correlations. The importance of the experimental discovery was highlighted with a Nobel prize for H. Störmer and D. Tsui in 1998 jointly with R. Laughlin [7–9], whose seminal work explained the initial experimental observations. This theory had a profound influence on the rapid developments in our understanding of the effect which subsequently followed, as it opened up the whole field for exploration [10]. In this review, we will however demonstrate that it is essential to go beyond the Laughlin approach in order to understand a very fundamental property of the FQHE system, namely, various spin transitions at several primary filling factors. From early theoretical works and the supporting experimental evidences (old and new), it has now been well established that the states at $\nu = \frac{2}{3}$, $\nu = \frac{4}{3}$, $\nu = \frac{2}{5}$ and $\nu = \frac{8}{5}$ begin with a spin-singlet ground state at low magnetic fields. As the magnetic field is increased there is a rather sharp transition to a fully spin-polarized ground state. Recent experimental results indicate that these transitions are of first-order type. Spin reversed states are also apparent at $\nu = \frac{3}{5}$, the existence of which was predicted in earlier theoretical calculations. Similarly, spin-reversed excitations, rather than Coulomb-driven quasiparticle–quasihole excitations, which are predicted to exist under suitable conditions and manifest themselves by the linear magnetic field dependence of the energy gap, are established in various experiments as well.

In section 2, we present, in a nutshell, the early days of the development of the FQHE and then gradually move into the domain of spin effects in the system. We present a systematic picture of the developments of our understanding of the spin degree of freedom in QHE and describe how various experiments have offered a clear means to visualize these spin effects. A detailed account of the results of tilted-field experiments at various filling factors is given in this section. Similarly, a detailed theoretical picture of various spin-reversed ground states and the spin-reversed quasiparticles is also presented.

Section 3 describes more recent experimental and theoretical results. These include nuclear magnetic resonance, optical spectroscopy, and the observation of novel effects like hysteresis, the huge longitudinal resistance maximum, etc, which are direct reflections of spin transitions in the system. Spin excitations near a filled Landau level, including skyrmionic excitations, are also briefly discussed.

The review concludes with a brief look at the open questions and theoretical challenges which need to be faced in the near future.

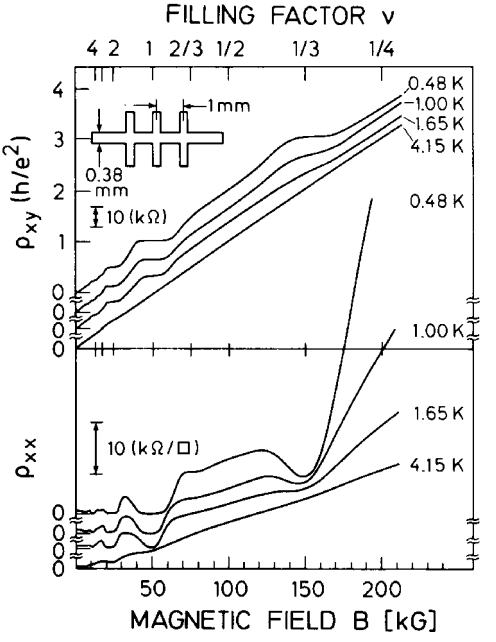

Figure 1. The very first result of the FQHE at 1/3 filling of the lowest Landau level [1].

2. Early work

The fractional quantum Hall effect was experimentally realized in high-mobility two-dimensional electron gas (2DEG) in $GaAs/Al_xGa_{1-x}As$ heterostructures [1, 3–5]. It is chracterized by the fact that the Hall conductance has plateaus quantized to certain simple *fractions* ν of the unit e^2/h and at the same value of the magnetic field, longitudinal resistivity shows an almost dissipationless current flow. Here ν is a rational fraction with an odd denominator†. Early results of the discovery are displayed in figure 1. For $\nu > 1$, the characteristic features of the integral QHE are clearly visible in this figure‡. In the extreme quantum limit, i.e. for $\nu < 1$ and at low temperatures, one observes a clear minimum in ρ_{xx} and a quantized Hall plateau at $\nu = \frac{1}{3}$. Later, in more refined experiments [12–14] these effects at several other fractions were observed which are displayed in figure 2 and summarized below:

$\frac{1}{3}$	$\frac{1}{5}$	$\frac{1}{7}$	$\frac{2}{5}$	$\frac{2}{7}$	$\frac{2}{9}$	$\frac{2}{11}$	$\frac{3}{7}$	$\frac{3}{11}$	$\frac{3}{13}$	$\frac{3}{17}$	$\frac{4}{9}$	$\frac{4}{11}$	$\frac{4}{13}$	$\frac{5}{11}$	$\frac{6}{13}$	$\frac{7}{15}$
$\frac{2}{3}$	$\frac{4}{5}$	$\frac{3}{5}$	$\frac{5}{7}$	$\frac{4}{7}$	$\frac{5}{9}$	$\frac{6}{11}$	$\frac{7}{13}$								
$\frac{4}{3}$	$\frac{7}{5}$	$\frac{9}{7}$	$\frac{5}{3}$	$\frac{8}{5}$	$\frac{10}{7}$	$\frac{13}{9}$	$\frac{11}{7}$	$\frac{7}{3}$	$\frac{8}{3}$	$\frac{5}{2}$						

Some of the fractions have as yet shown structures in ρ_{xx} only. The first row of fractions are simply $\nu = p/q (2p < q)$. The second row contains the fractions $\nu = 1 - p/q$ and the last row contains the other fractions $\nu = 1 + p/q$,

† In fact, an even denominator fraction has also been found to exhibit the FQHE [11, 12].

‡ A very lucid account of early experiments leading to the discovery of FQHE has been presented by Störmer in Reference [7].

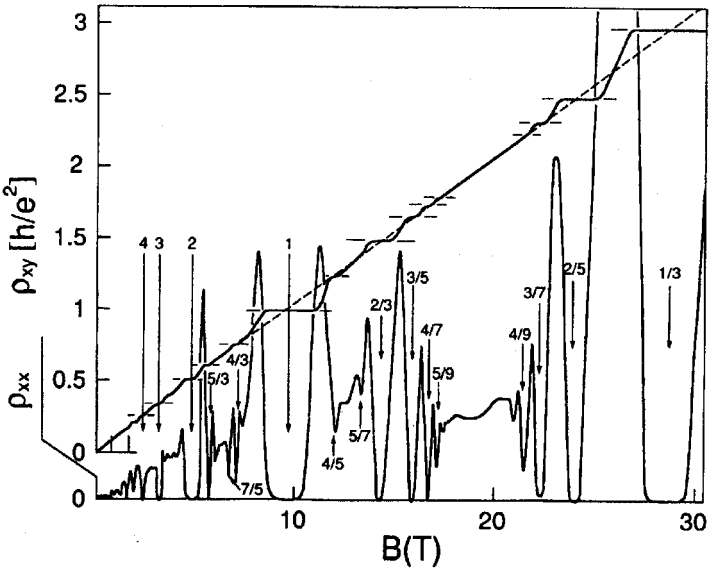

Figure 2. Overview of the observed fractions in the FQHE measurements.

$1+(1-p/q), 2+p/q$, etc. The major characteristics of FQHE, namely, the appearence of plateaus in ρ_{xy} and minima in ρ_{xx}, are similar in nature to those of the IQHE. However, the physical origin of the FQHE need to be different from that of IQHE because

(1) plateaus and minima appear at *fractional* filling factors where no structure is expected in the single-particle density of states, and
(2) the effect is observed only in samples of very high mobility.

These facts lead to a natural conclusion that electron–electron interaction plays a major role in the effect. Therefore, immediately after the experimental discovery a major task for theoreticians was to determine the properties of an interacting 2DEG with a neutralizing background subjected to a strong perpendicular magnetic field such that only the lowest Landau level is partially filled. Among the various attempts to solve this problem, the most successful theory in 1983 was that of Laughlin [10] who established that the ground state at $\nu = \frac{1}{3}$ is a translationally invariant liquid. He also explained the mechanism behind the exceptional stability of the $\frac{1}{3}$ state.

2.1. *Laughlin's wavefunction: the beginning*

The best source for understanding Laughlin's approach is, of course, his own articles [8, 10, 15]. A detailed version of this theory and its various outcomes is available in [16, 17]. In this theory, electrons are confined in the xy plane which is taken to be a complex plane with $z = x - \mathrm{i}y$ being the electron position. In a symmetric gauge with a vector potential, $\mathbf{A} = \frac{1}{2}(x\hat{y} - y\hat{x})$, the single-particle wave functions (unnormalized)

$$\varphi_m \equiv |m\rangle \sim (z/\ell_0)^m \exp(-|z|^2/4\ell_0^2) \tag{1}$$

are eigenfunctions of the orbital angular momentum. Here, $\ell_0 \equiv (\hbar c/eB)^{1/2}$ is the cyclotron radius in the lowest Landau level—the magnetic length. Some important

results readily follow from (1). The degeneracy of a Landau level $n_s = A/2\pi\ell_0^2$, A being the area of the system, is the upper bound to the quantum number m. This is seen by requiring that $\pi\langle r^2\rangle \leq A$. The area covered by a single electron in state $|m\rangle$, moving in its cyclotron orbit is, in fact, proportional to m: $\langle m|r^2|m\rangle = 2(m+1)\ell_0^2$ (including the appropriate normalization factor [16–18] in (1)). This then leads to $m \leq n_s - 1$. Therefore, the state space of an electron in the lowest Landau level is spanned by $1, z, z^2, \ldots, z^{n_s-1}$ times the exponential factor $\exp(-|z|^2/4\ell_0^2)$.

The *Jastrow-type* many-electron (spin polarized) wave function proposed by Laughlin [10] for the $\nu = 1/m$ state is

$$\psi_m = \prod_{\substack{j,k=1 \\ j<k}}^{n_e} (z_j - z_k)^m \prod_{j=1}^{n_e} \exp(-|z_j|^2/4\ell_0^2). \tag{2}$$

When m is an odd integer, this wave function obeys Fermi statistics. The wave function is entirely made up out of states in the lowest Landau level. It is also an eigenstate of the angular momentum with eigenvalue $M = \frac{1}{2}n_e(n_e - 1)m$. The total angular momentum M is the degree of the polynomial (conservation of angular momentum). Let us expand the first product in powers of z_1, keeping all the other coordinates fixed. The highest power of z_1 is then $m(n_e - 1)$ which, from the arguments above, must be $(n_s - 1)$. For large n_e, it then follows that $m \approx \frac{1}{\nu}$ [16]. For $m = 1$ (filled Landau level), the polynomial $\prod_{j<k}(z_j - z_k)$ is the Vandermonde determinant of order n_e. As $n_e \to \infty$, the particle density in this state tends to $(2\pi\ell_0^2)^{-1}$ [19]. The Laughlin state for $m = 1$ is the exact ground state for a filled Landau level.

The Laughlin state (2) has a very interesting property, i.e. when one electron is adiabatically moved while the position of all the other electrons are held fixed, the $m(n_e - 1)$ zeros are attached to the position of the other electrons. The m-fold vanishing of the wave function when two electrons come close helps to keep the electrons away from each other. Halperin pointed out that the Laughlin wave function makes optimum use of the zeros by placing them directly at the position of the electrons and thereby reduces the Coulomb energy of the system [20]. There are no *wasted* zeros in the system. At the same time, the wave function (2) describes a state where m flux quanta of applied magnetic flux are bound to each electron, which leads to the filling factor of $\nu = 1/m$. A slight deviation of the density from $\nu = 1/m$ can be achieved by having additional zeros (or flux quanta) in the system not tied to any electron. This would generate the fractionally-charged quasiholes and quasiparticles—the elementary excitations in the system proposed by Laughlin [10]. The energy cost to create these elementary excitations, i.e. the energy gap, essential to explain the fractional quantization of the Hall effect, keeps the system pinned at the density corresponding to $\nu = 1/m$.

Although the form of wave function (2) could have been anticipated before Laughlin's work, especially, after the work of Bychkov *et al.* [19] at $\nu = 1$, any practical use of the function was not immediately apparent. This is because of the explicit dependence of the wave function on the particle position. The steps that were needed to circumvent this problem were entirely due to Laughlin's brilliant idea of mapping the system described by this wave function on a two-dimensional, charge-neutral classical plasma [16, 17]. This mapping not only provided a means to calculate the ground-state energy and correlation function, it also provided a robust

picture of the liquid state. It provided explanations for (i) uniform density of the liquid state, (ii) incompressibility of the system, and (iii) showed how one can calculate the quasiparticle and quasihole creation energies [16, 17]. The fundamental ideas of Laughlin's theory, like the incompressibility, zeros bound to electrons, etc., still remain the cornerstones for all other approaches [21, 22] to explore the unique properties of incompressible, correlated electron systems in a magnetic field [16].

While details of Laughlin's mapping of the electron system onto a classical plasma can be found in [16], let us briefly mention here some of the points pertinent to our present review. In this approach, one writes the probability distribution

$$|\psi_m|^2 = \exp(-\mathcal{H}_m),$$
$$\mathcal{H}_m = -2m \sum_{j<k} \ln |z_j - z_k| + \sum_j |z_j|^2 / 2\ell_0^2,$$

where $\mathcal{H}_m$ is readily recognized as the Hamiltonian for a charge neutral 2D classical plasma with logarithmic interparticle interaction and an uniform neutralizing background with particle density $\rho_m = 1/2\pi\ell_0^2 m$. The plasma maintains its charge neutrality by spreading out *uniformly* with density ρ_m (i.e. $\nu = 1/m$). From the vast literature of classical plasma (see, for example, [23, 24]), Laughlin was able to extract the relevant properties that are applicable to his 2D electron system, namely, the pair-correlation function, the ground-state energy, and a very important fact that the system is a translationally invariant *liquid* for $m = 3, 5, \ldots$ [16].

In order to obtain densities slightly different from $\nu = 1/m$, we can add a few extra zeros not tied to electron positions i.e. $\nu < 1/m$. One then creates Laughlin's *quasihole* excitations given by the state

$$\psi_m^{(-)} = \exp\left(-\tfrac{1}{4}\sum_l |z_l|^2\right) \prod_j (z_j - z_0) \prod_{j<k} (z_j - z_k)^m, \tag{3}$$

where $z_0 = x_0 - \mathrm{i}y_0$. State (3) has a simple zero at $z = z_0$ for any j, as well as m-fold zeros at each point where $z_j = z_k$, for $k \neq j$. The plasma Hamiltonian in this case is that of a classical one-component plasma with an extra phantom point charge at z_0 whose strength is *less* by a factor $1/m$. The plasma will neutralize the phantom by a ***deficit*** of $1/m$ charge near z_0. Elsewhere in the interior of the plasma the charge density remains unchanged. The real electron system will have a net charge $-e/m$ accumulated in the vicinity of z_0 and a quasihole excitation is created. A somewhat similar situation can be thought of for the fractionally-charged quasiparticles. For details about the calculation of quasihole and quasiparticle creation energies, as well as a comparison with the experimental results for the energy gap, see [16]. Direct detection of the fractional charge $(e/3)$ of Laughlin quasiparticles has been reported recently [25].

Laughlin's theory at $\nu = 1/m$, $m \rightarrow$ odd integer, cannot be directly applied to the case of m being an *even* integer because in that case the wave function (equation (2)) describes a system of particles obeying Bose statistics. Efforts are under way to generalize the Laughlin wave function where Fermi statistics is properly included [26, 27], but the suitability of that approach is still unclear. Since the state at $\nu = \frac{1}{2}$ is a very enigmatic case, it has received a lot of attention lately [26–31]. A detailed description of this interesting problem is, however, beyond the scope of this review.

2.2. *Mixed-spin ground state*

At high magnetic fields and for large enough values of the g factor, all electrons are expected to have their spins aligned with the magnetic field and one can safely ignore the spin degree of freedom in the theory of FQHE. Halperin [20] was the first to point out a very important fact, i.e. the g factor for electrons in GaAs is about a quarter to that of the free electron value but $1/m^*$ is large. This leads to a very small Zeeman energy relative to the cyclotron energy. Therefore the usual assumption of full spin polarization at all filling factors is worth a re-examination. He proposed that a Laughlin-like but *spin-unpolarized* state can be constructed at $\nu = 2/(m+n)$

$$\psi = \prod_{j<k}(z_j - z_k)^m \prod_{\alpha<\beta}(z_\alpha - z_\beta)^m \prod_{j,\alpha}(z_j - z_\alpha)^n \prod_j \exp(-|z_j|^2/4\ell_0^2) \prod_\alpha \exp(-|z_\alpha|^2/4\ell_0^2), \tag{4}$$

where Roman and Greek indices correspond to electrons with two different spin states†. The ground-state energy of the $\nu = \frac{2}{5}(m = 3, n = 2)$ state, calculated for the first time by Chakraborty and Zhang [32] using the two-component classical plasma approach [16], was $E_{\text{unpol}} = -0.434e^2/\epsilon\ell_0$. When compared with the ground-state energy of the fully spin polarized state, $E_{\text{pol}} \approx -0.4303 \pm 0.003e^2/\epsilon\ell_0$ [33] it is clear that the fully spin-polarized state is not always favoured energetically, especially when the Zeeman energy is vanishingly small. With this result a very intriguing possibility to observe a spin-reversed FQHE ground state was thereby established for the first time. It indicated that although at high magnetic fields (or a non-zero g factor) the Zeeman energy will stabilize the polarized state, there always exists a possibility for a transition to an unpolarized state at lower fields (or vanishingly small g values, as described below)‡. Immediately after this work, a systematic study of spin polarizations in the ground state at various filling factors was undertaken by Zhang and Chakraborty [35], using a method which was to become a very popular tool for studying the QHE in later years. The method involves exact diagonalization of a few-electron Hamiltonian in a magnetic field and in a suitable geometry (in this particular case, the periodic rectangular geometry). A brief description of the method is given below.

Let us consider a system of n_e electrons in a rectangular cell in the xy plane with periodic boundary conditions [16, 36]. The area of the cell is $a \times b$. In the Landau gauge, the single-electron wave function is given by

$$\varphi_{n_L j}(\mathbf{r}) = \left(\frac{1}{2^{n_L} n_L! \pi^{1/2} b \ell_0}\right)^{1/2} \sum_{k=-\infty}^{\infty} H_{n_L}\left[(k_y - x)\ell_0\right] \exp\left[ik_y y/\ell_0^2 - (k_y - x)^2/2\ell_0^2\right]. \tag{5}$$

Here $k_y = X_j + ka$, the integer j ($1 \le j \le n_s$) specifies the state and $X_j = (2\pi\ell_0^2/b)j$ is the centre coordinate of the cyclotron motion which is conserved by the electron–electron interaction. $H_{n_L}(x)$ is the Hermite polynomial and n_L is the Landau quantum number. The area of the cell is fixed to $ab = 2\pi\ell_0^2 n_s$, where n_s is an integer which is the degeneracy of a single Landau level and the ***filling factor*** is $\nu = n_e/n_s$. In

† In later years, this two-spin state became very popular as a state describing a two-layer system, albeit at *zero* separation of the layers.

‡ A brief but comprehensive review of spins in the QHE is available in Reference [34].

the lowest Landau level ($n_L = 0$) the Hamiltonian is written in the second quantized form as

$$\mathcal{H} = \mathcal{E}_0 \sum_{j,\sigma} a^\dagger_{j\sigma} a_{j,\sigma} + \sum_{j_1 j_2 j_3 j_4 \sigma,\sigma'} \mathcal{A}_{j_1 j_2 j_3 j_4} a^\dagger_{j_1,\sigma} a^\dagger_{j_2\sigma'} a_{j_3,\sigma'} a_{j_4,\sigma},$$

where the single-electron term is the result of the interaction between an electron and its image and therefore, $\mathcal{E}_0$ is the classical Coulomb energy of a Wigner crystal with rectangular unit cell [37] which depends only on the cell geometry. The two-electron term of the Hamiltonian where we consider the Coulomb interaction is given by

$$\mathcal{A}_{j_1 j_2 j_3 j_4} = \delta'_{j_1 + j_2, j_3 + j_4} \mathcal{F}(j_1 - j_4, j_2 - j_3), \tag{6}$$

$$\mathcal{F}(j_a, j_b) = \frac{1}{2ab} \sum_{\mathbf{q}}{}' \sum_{k_1,k_2} \delta_{q_x, 2\pi k_1/a} \delta_{q_y, 2\pi k_2/b} \delta'_{j_a, k_2} \times \frac{2\pi e^2}{\epsilon q} F(q) \exp\left(\tfrac{1}{2} q^2 \ell_0^2 - 2\pi i k_1 j_b / n_s\right).$$

For a pure two-dimensional system $F(q) = 1$, but it is different from unity when we consider below the finite width of the electron wave function perpendicular to the electron plane. In equation (6), the summation over q excludes $q_x = q_y = 0$ and the Kronecker delta with the prime means that $\delta'_{j_1 j_2} = 1$ when $j_1 = j_2 \pmod{n_s}$, and $\mathbf{q} = ((2\pi/a)n_1, (2\pi/b)n_2)$, where n_1 and n_2 are integers. The basis states are chosen to be the antisymmetrized products of single-particle eigenfunctions (equation (5)) denoted by $|j_1, j_2, \ldots, j_{n_e}\rangle$, with the quantum number $J \equiv \sum_{i=1}^{n_e} j_i \pmod{n_s}$ being the total momentum along the axis fixed by the Landau gauge. It is interesting to note that according to the particle–hole symmetry in a Landau level, one has $\nu \leftrightarrow 1 - \nu$ for spinless electrons and $\nu \leftrightarrow 2 - \nu$ otherwise. The latter case was first pointed out in [38]. This correspondence rule, which ignores Landau level mixing, is, as we shall demonstrate below, a very good assumption in order to explain many of the experimental results for a two-dimensional electron gas. *A priori* it is not obvious that a similar result would hold for a two-dimensional hole gas, created either in a p-type GaAs heterojunction [39–41] or in a quantum well structure [42–44]. Here, because of the heavier hole mass, Landau levels are much more closely spaced. Moreover, the spin–orbit interaction invalidates the distinction between the spin gap and the cyclotron gap. Fortunately, experimental results on two-dimensional hole systems, described below, indicate that the correspondence rule holds for the hole system equally well. The electron–hole symmetry, as explained above, is therefore quite robust.

The total energy of n_e two-dimensional (2D) interacting electrons consists of two terms: (i) the Coulomb term, which depends on the total spin $|S|$ and the perpendicular component of the external magnetic field, and (ii) the Zeeman term $E_z = g\mu_B B S_z$, where g is the Landé g factor for electrons in the medium and μ_B is the Bohr magneton. A fully spin-polarized state corresponds to $|S| = n_e/2$. An unpolarized state corresponds to $|S| = 0$ for n_e even and $\frac{1}{2}$ for n_e odd. Any other values of $|S|$ would correspond to a partilally polarized state.

Existence of spin unpolarized states in low magnetic fields at $\nu = \frac{2}{3}$ and the corresponding electron–hole symmetric $\nu = \frac{4}{3}$ state was first pointed out by Maksym [45] in finite-size calculations in a periodic rectangular geometry. He argued that the spin transitions are the result of competition between Coulomb repulsion, exchange

Table 1. Ground-state energy per particle for various filling factors and ground-state spin polarizations. The Zeeman energy is not included in the energy values which are in units of $e^2/\epsilon\ell_0$. The $\nu = \frac{1}{3}, \frac{2}{5}$ results are for a four-electron system and $\nu = \frac{2}{3}, \frac{3}{5}$ are for a six-electron system. For incompressible states, the ground-state energy is rather insensitive to the system size [16]. The experimental results for these filling fractions are now available and they are discussed in section 2.6.

	Ground-state energy				
ν	$S=0$	$S=1$	$S=2$	$S=3$	Ground state
$\frac{1}{3}$	-0.4135	-0.4120	-0.4152	—	Polarized
$\frac{2}{3}$	-0.5331	-0.5291	-0.5257	-0.5232	Unpolarized
$\frac{2}{5}$	-0.4464	-0.4410	-0.4403	—	Unpolarized
$\frac{3}{5}$	-0.5074	-0.5096	-0.5044	-0.50104	Partially polarized

and interaction of unlike spins. In the case of filling factors $\nu = \frac{2}{3}, \frac{2}{5}$, and other filling factors, similar conclusions about the nature of spin polarizations were also reported by several other authors [46, 47]

From the discussions above the following results have emerged (table 1): at zero, or very low Zeeman energies, the preferred spin states at the ground states of the major fractions are as follows:

(1) $\nu = \frac{1}{3}$ and $\nu = \frac{5}{3}$ (electron–hole symmetric) are fully polarized;
(2) $\nu = \frac{2}{3}, \frac{2}{5}$ and $\nu = \frac{4}{3}, \frac{8}{5}$ (electron–hole symmetric) are spin unpolarized;
(3) $\nu = \frac{3}{5}$ and $\nu = \frac{7}{5}$ (electron–hole symmetric) are partially polarized.

Experimental verifications of these predictions of various spin polarizations is discussed in section 2.6. It is interesting to note that the ground state at $\nu = \frac{1}{3}$ is fully spin polarized even in the absence of Zeeman energy (inclusion of Zeeman energy would make this state even more favourable relative to other spin states). This is in line with the fully antisymmetric wave function of Laughlin discussed above. At other filling factors, spin-reversed ground states are possible for vanishingly small Zeeman energy. As we shall see below, many of these predicted spin states have been observed in experiments. In figure 3, we present the results for the ground-state energy (per particle) for (*a*) $\nu = \frac{2}{5}$ and (*b*) $\nu = \frac{2}{3}$ where the Zeeman energy ($g = 0.4$) contributions are included [48]. In both cases, a crossover magnetic field B_c was observed, below which a spin-unpolarized state is energetically favoured. The fully spin-polarized state is favoured for magnetic fields above the crossover magnetic field B_c. In order to evaluate B_c for a more realistic system, one should include corrections owing to finite thickness of the 2DES and the Landau level mixing, to be discussed below.

2.2.1. *Finite-thickness corrections*

An important correction to the ground-state energy and the excitation energy is to consider the finite width of the electron wave function perpendicular to the electron plane. Here usually one considers a variational wave function in the z direction (where only the lowest subband is considered) of the form [49, 50]

$$\psi(z) = \left(\tfrac{1}{2}d^3\right)^{1/2} z \exp(-dz/2), \tag{7}$$

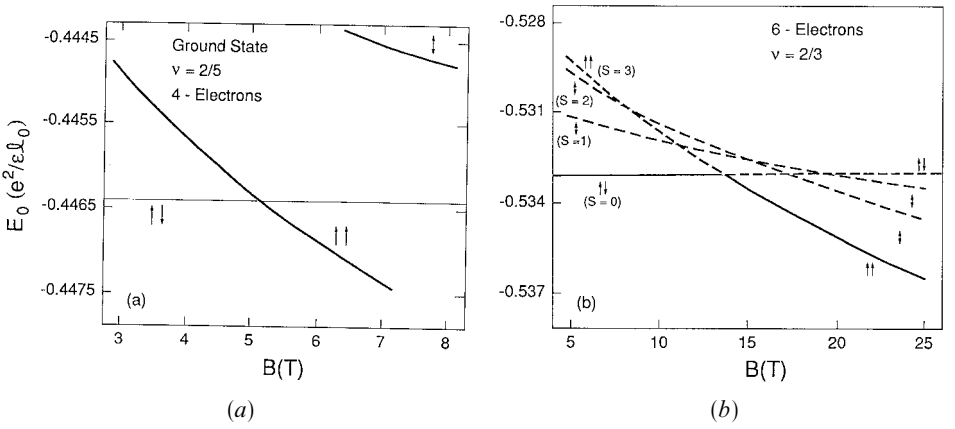

(*a*) (*b*)

Figure 3. Ground state energy per particle (in units of $e^2/\epsilon\ell_0$) versus B (tesla) for (*a*) $\nu = \frac{2}{5}$ and (*b*) $\nu = \frac{2}{3}$ for different spin polarizations: fully spin polarized ($\uparrow\uparrow$), spin unpolarized ($\uparrow\downarrow$) and partially spin polarized ($\updownarrow$). The dashed lines correspond to energetically unfavoured regions [48].

where d is the variational parameter which depends on the sample parameter (effective mass, electron density, etc.). The case of a true two-dimensional system corresponds to $d = \infty$. For a non-zero width of the electron plane the function $F(q)$ in equation (6) is modified as

$$F(q) = \frac{8 + 9(q/d) + 3(q/d)^2}{8(1 + q/d)^3}, \tag{8}$$

whose major effect is to soften the short-range divergence of the bare Coulomb interaction, when the interelectron spacing is comparable with the inversion layer width. As a result, many important energies in the FQHE are sharply reduced [16, 51]. In the calculations that follow, the parameter $\beta = (d\ell_0)^{-1}$ determines the three-dimensionality of the system†. Figure 4 depicts the ground-state energy of the Laughlin state and is seen to be reduced drastically as a result of the finite-thickness correction [16].

2.3. *Spin-reversed quasiparticles*

After it was theoretically established that under certain conditions various FQHE ground states are spin unpolarized, it was quite natural to inquire if the lowest-lying excitations also involve spin flip. The energy gap, $E_g = \varepsilon_p + \varepsilon_h$, which corresponds to the energy required to create a quasiparticle (ε_p) and a quasihole (ε_h) well separated from each other, was estimated by several authors [33, 52–56]. Results of the exact diagonalization scheme for finite electron systems in a periodic rectangular geometry by Chakraborty *et al.* at $\nu = \frac{1}{3}$ [57, 58] are shown in figure 5 as solid lines with open or filled points. Finite-thickness corrections and Zeeman energy (in K) $\varepsilon_Z = 0.535B$ (B in tesla) are already included in these results. At low fields, the lowest energy excitation, which corresponds to spin-reversed quasiparticles and spin polarized

† For B measured in tesla, $\beta \sim 0.525B^{1/6}$, at $\nu = \frac{1}{3}$ and $\beta \sim 0.416B^{1/6}$ at $\nu = \frac{2}{3}$ for parameters appropriate to GaAs heterostructures.

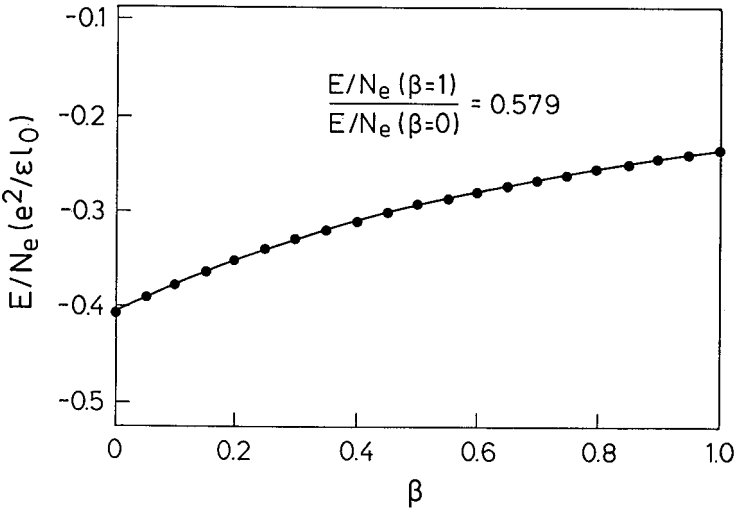

Figure 4. Ground-state energy per particle as a function of the dimensionless thickness parameter $\beta = (d\ell_0)^{-1}$ for the Laughlin wave function.

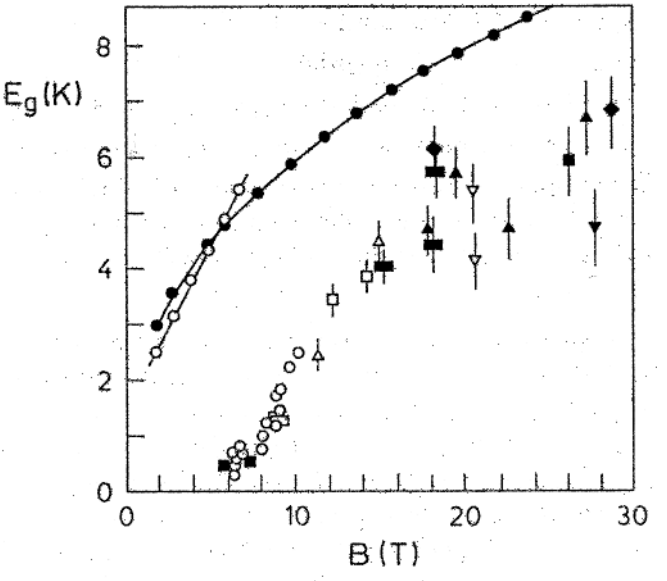

Figure 5. Theoretical results (upper two curves): calculated energy gap E_g (K) versus magnetic field B (T) for a five-electron system. Open circles are for spin reversed quasiparticles and spin polarized quasiholes and filled circles are for the fully spin polarized case. Experimental data of [59] (open and filled symbols): Activation energy (K) as a function of magnetic field. Open symbols are the data for $\nu = \frac{2}{3}$. Filled symbols are for $\nu = \frac{1}{3}$, except for two filled squares at 5.9 and 7.4 T which are for $\nu = \frac{5}{3}$ and $\frac{4}{3}$.

quasiholes, rises *linearly* because of the dominant contribution of Zeeman energy. As the magnetic field is increased further, a crossover point is reached beyond which a fully polarized quasiparticle–quasihole state is energetically favoured, and correspondingly, we obtain the $B^{1/2}$ dependence (modified by the magnetic field dependence of β). In fact, the very possibility of linear field dependence of the gap (in

contrast to the $B^{1/2}$ dependence of a Laughlin quasiparticle gap) and its association with Zeeman energy was first emphasized in [57, 58] and subsequently observed in experiments (see sections 2.6 and 3.4).

In figure 5, we compare our theoretical results for the energy gap with the activation energy data by Boebinger *et al.* [59] who reported a systematic study of the energy gap for the filling fractions $\nu = \frac{1}{3}, \frac{2}{3}, \frac{4}{3}$ and $\frac{5}{3}$. The energy gap is usually derived from the measured temperature dependence of the magnetoconductivity: σ_{xx} (or ρ_{xx} since near the ρ_{xx} minima, $\rho_{xx} \ll \rho_{xy}$, and $\sigma_{xx} = \rho_{xx}/(\rho_{xx}^2 + \rho_{xy}^2) \sim \rho_{xx}/\rho_{xy}^2$), as $\sigma_{xx} \propto \rho_{xx} \propto \exp(-W/k_B T)$, where $W = \frac{1}{2}E_g$ is the activation energy and k_B is Boltzmann's constant. The remarkable behaviour in these experimental results is the *linear* increase of the activation data for $\nu = \frac{2}{3}$ (open symbols), and a somewhat modified $B^{1/2}$ behaviour at high fields, not unlike the theoretical results discussed above.

Calculation of the charge density profiles at $\nu = \frac{1}{3}$ revealed [38] that the spin-reversed excitation has a localized fractional charge of $\frac{1}{3}$, the same as for the excitation without spin reversal. The density profile of the spin-reversed excitation show that the spin-reversed electron is localized around the centre of the defect, which is a spin-1 object with a fractional charge of $\frac{1}{3}$. The energy gain in a spin-reversed excitation, as opposed to a spin-0 excitation, is explained as the result of less energy being required to accumulate the charge at the defect.

For an infinite system, Morf and Halperin [33] proposed the following trial wave function for spin-reversed quasiparticles

$$\psi_q = \prod_{j=2}^{n_e} (z_j - z_1)^{-1} \psi_L, \tag{9}$$

where ψ_L is the Laughlin state. Using the classical plasma analogy, they argued that $|\psi_q|^2$ is the distribution function for a two-dimensional plasma in which particle 1 has its charge *reduced* by a factor $[1 - (1/m)]$ in its repulsive interaction (in the corresponding plasma Hamiltonian) with the other particles. Particle 1 has, however, the same attractive interaction with the background as the other particles. Particle 1 will therefore be attracted to the centre of the disc, while a two-dimensional *bubble* will be formed near the origin of size $[1 - (1/m)]$. As a result, there will be an extra negative charge e/m near the origin. A two-component plasma calculation was performed by Chakraborty [60] to demonstrate that this wave function indeed has the lowest energy in the absence of Zeeman energy.

It is interesting to note that for a number n_q of spin-reversed quasiparticles in the Laughlin state at $\nu = 1/m$, a trial wave function can be written as [38]

$$\psi(z_1, \ldots, z_{n_e}) = \prod_{i<j}^{n_e} (z_i - z_j)^{m-1+\delta_{\sigma_i \sigma_j}} \exp\left[-\frac{1}{4\ell_0^2} \sum_{i=1}^{n_e} |z_i|^2\right], \tag{10}$$

where $\sigma_i = -1$ for $i = 1, \ldots, n_q$ and $\sigma_i = 1$ for $i = n_q + 1, \ldots, n_e$, z_i is, as usual, the complex coordinate of the ith electron. Let us now consider the following two cases: (a) $n_q = 1$ and (b) $n_q = \frac{1}{2}n_e$. In the former case, we have the state containing just one spin-reversed quasiparticle and (10) reduces to state (9). In case (b), we have the spin unpolarized state at $\nu = 2/(2m-1)$ and equation (10) reduces to the state equation (4) discussed in section 2.2.

The spin-reversed quasiparticle (qp)–quasihole (qh) gaps for two different ground states (spin-unpolarized and fully spin polarized) at $\nu = \frac{2}{5}$ are depicted in figure 6 (*a*).

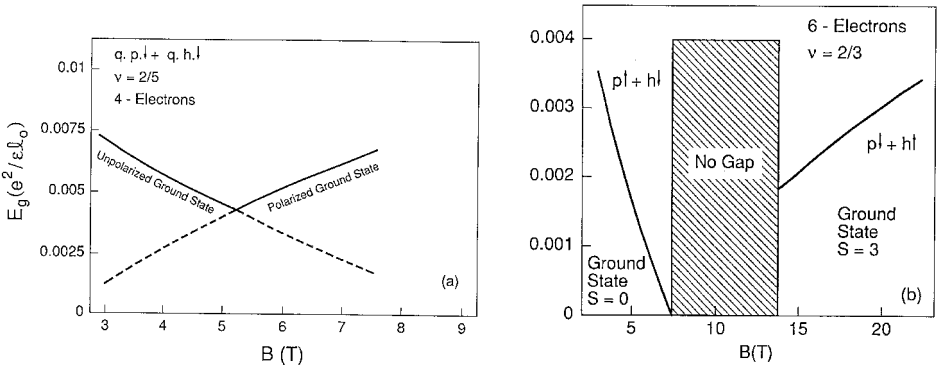

(*a*) (*b*)

Figure 6. Lowest energy quasiparticle–quasihole gap (in units of $e^2/\epsilon\ell_0$) as a function of magnetic field B (in tesla) for (*a*) $\nu = \frac{2}{5}$ and (*b*) $\nu = \frac{2}{3}$. Above and below the crossover point, two different ground states from figure 3 are considered. The gap is non-existent in the shaded region as discussed in the text [48].

These are the lowest energy excitations in the presence of Zeeman energy†. The sharp change in slope is similar to the *re-entrant* behaviour observed in activation energy measurements at $\nu = \frac{8}{5}$ to be discussed below. The excitations were identified here as the spin-reversed qp–qh pair [48].

The results for the qp–qh gap for $\nu = \frac{2}{3}$ are depicted in figure 6(*b*). Just as in figure (*a*), we plot only the lowest energy excitations as a function of the magnetic field, with the Zeeman energy included. In this case, the situation is clearly different from that of $\nu = \frac{2}{5}$. Below the crossover point the preferred ground state is spin-unpolarized. The lowest energy excitations in this state involve a spin-polarized qp-spin-reversed qh pair. The energy gap decreases rapidly and vanishes before the crossover point is reached. From this point onward the discontinuity in the chemical potential is in fact negative, indicating that FQHE is unstable in this region of the magnetic field. Beyond the crossover point, the spin-unpolarized state is no longer the ground state and the energy gap is to be calculated from the fully spin-polarized ground state. In this case spin-reversed qp-spin-polarized qh pair-excitations have the lowest energy and the energy gap steadily increases with the magnetic field. Therefore, between the two ground states exhibiting FQHE there is a *gapless domain* where the FQHE state is not stable. Such a gapless domain is not present at $\nu = \frac{2}{5}$. Similar gapless regions and much more complicated structures in the magnetic field dependence of the quasiparticle–quasihole gap were predicted theoretically for other higher-order filling factors [61].

One such interesting case is the filling factor $\nu = \frac{3}{5}$ [16, 61]. In figure 7, we present the results for the ground-state energy per particle for $\nu = \frac{3}{5}$ versus the magnetic field where the Zeeman energy ($g = 0.5$) is also included. The results are shown for three values of the total spin ($S = 1$, 2 and 3). Only two states (spin polarized ($\uparrow\uparrow, S = 3$) and partially polarized ($\updownarrow$), with $S = 1$) are found to provide the lowest energy with increasing magnetic field. The spin-unpolarized state ($S = 0$) is much higher in energy compared to the other two states and is not included in the figure. As for the $\frac{2}{5}$

† In figures 6–8 we use material parameters that are appropriate to GaAs heterostructures.

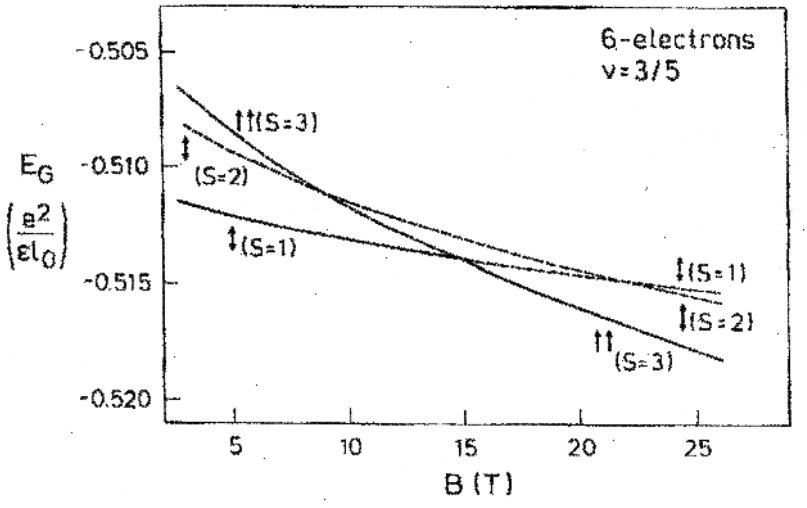

Figure 7. Ground-state energy per particle ($e^2/\epsilon\ell_0$) versus B (tesla) at $\nu = \frac{3}{5}$ for various spin polarizations; the fully polarized ($\uparrow\uparrow, S = 3$ and partially polarized $\updownarrow, S = 1,2$) spin states. The dashed lines in all the curves correspond to the energetically unfavoured regions [61].

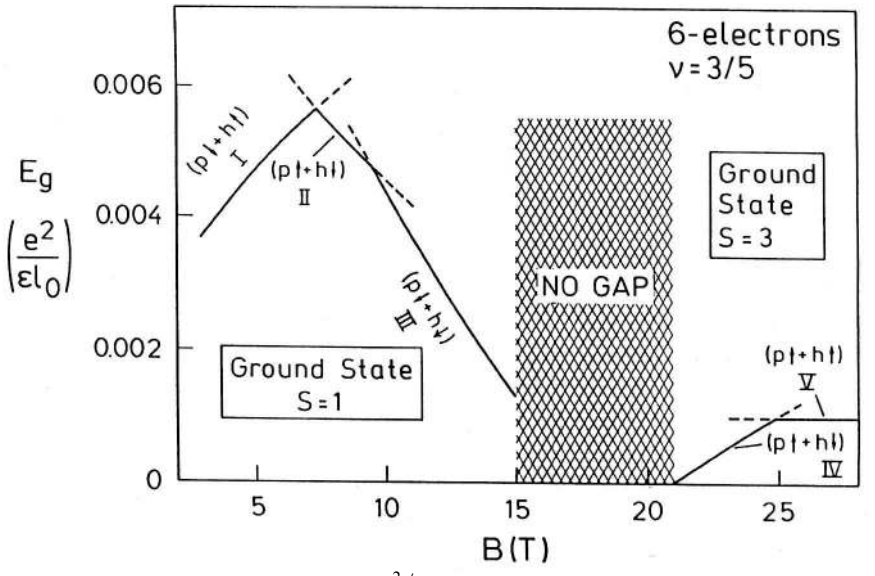

Figure 8. Quasiparticle–quasihole gap ($e^2/\epsilon\ell_0$) versus the magnetic field B (tesla) at $\nu = \frac{3}{5}$ for various spin polarizations in two different ground states. The shaded region indicates that the gap is non-existent there, as discussed in the text. The regions I–V are also explained in the text [61].

state, we observe a crossover point in the magnetic field below which the partially polarized spin state is energetically favoured. The fully polarized spin state is favoured for magnetic fields beyond the crossover point.

The results for the qp–qh gap (in units of $e^2/\epsilon\ell_0$) versus the magnetic field are presented in figure 8. The Zeeman energy contribution has been included in these results. At low magnetic fields (up to $\sim$7.5 T), the spin-reversed qp–spin-polarized qh

gap is found to have the lowest energy (region I). With increasing magnetic fields, for a short range of magnetic fields (up to ~9.5 T) the spin-reversed qh–spin-polarized qp gap is favoured energetically (region II). For a further increase of the magnetic field up to the crossover point (region III), a spin-reversed qp–qh gap is found to have the lowest energy. In the region of magnetic field beyond the crossover point, the spin-partially-polarized state is no longer the ground state and the energy gap is to be calculated from the fully spin-polarized ground state. In this state for $15 \leq B \lesssim 21$ T, the gap is, in fact, first *negative* for a few values of B and then vanishingly small, indicating that the FQHE is no longer observable here. The energy gap is, however, found to reappear beyond 21 T (region IV), first with the spin-reversed qh–spin-polarized qp gap and eventually, for $B \gtrsim 25$ T (region V), a fully spin-polarized qp–qh gap appears to have the lowest energy. The fully spin-polarized gap is quite expected given the very high magnetic fields in this region. But the existence of spin-reversed excitations prior to this region is quite surprising.

In regions I–III, considering the different Zeeman energy contributions for different spin polarizations of qps and qhs, the novel transitions should be observable. The activation energy is expected to be linear in all three states, but the slopes will be different because of the different Zeeman energies. The activation energy in region IV will also be linear while that in region V does not have a Zeeman contribution and hence a $B^{1/2}$ behaviour is expected. Experimental investigation of the activation energy at this filling fraction should be able to distinguish the spin-reversed qp state from the spin-reversed qh state.

Rezayi investigated the FQH states at $\nu = \frac{1}{3}$ and $\nu = \frac{2}{5}$ by finite-size numerical calculations in a spherical geometry allowing reversed spins [62]. He found that the spin-reversed excitations can have, in general, lower energies, which may in some cases overcome the energy gap.

Morf and Halperin [63] numerically calculated the quasiparticle energy for the trial wave function equation (9) in a spherical geometry where one electron spin is reversed relative to the spin of all others. From their Monte Carlo calculations of systems containing up to 32 electrons they estimated the creation energy of a spin-reversed quasiparticle in the thermodynamic limit to be

$$\varepsilon_{\mathrm{qp}}^{\mathrm{s}} \approx 0.041 \pm 0.004 \, (e^2/\epsilon \ell_0)$$

(in the absence of Zeeman energy). Taking into account the finite width of the wave function in the z direction, their estimates were

$$\varepsilon_{\mathrm{qp}}^{\mathrm{s}} \approx \begin{cases} 0.0367, & \beta = \frac{1}{4}, \\ 0.0319, & \beta = \frac{1}{2}, \\ 0.0244, & \beta = 1. \end{cases}$$

These authors estimated that the crossover from spin reversed to spin polarized excitations would be at $B_{\mathrm{c}} \approx 7$ T.

2.3.1. *Landau level mixing*

The early work on the effect of Landau level mixing on the ground state was by Yoshioka [64] who concluded that the correction is insignificant for the Laughlin ground state at $\nu = \frac{1}{3}$. A Monte Carlo study of the $\nu = \frac{1}{3}$ FQHE state, in particular, the spin-polarized and spin-reversed quasiparticle energy gap, was reported recently

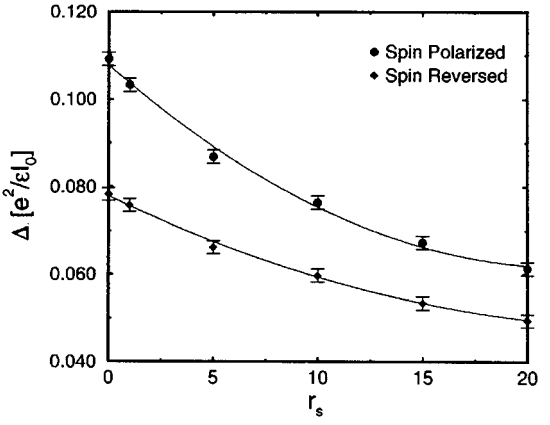

Figure 9. Monte Carlo results for the spin-polarized (•) and spin-reversed (◇) energy gaps at $\nu = \frac{1}{3}$ as a function of r_s, for a truely two-dimensional system [65, 66].

in [65, 66] where the influence of the Landau level mixing on the energy gap was also investigated. The latter correction was included as follows: in terms of the effective Bohr radius $a_B = \epsilon\hbar^2/m^*e^2$ and the mean interparticle spacing $r_0 = 1/(\pi n)^{1/2}$, the filling factor is written as $\nu = 2\ell_0^2/r_0^2$, and the electron gas parameter $r_s = r_0/a_B$. The degree of the Landau level mixing is expressed as $\left(e^2/\epsilon r_0\right)/\hbar\omega_c = r_s\nu/2$. Therefore, for a fixed ν, r_s gives a measure of the Landau level mixing. Since $r_s \propto m^*/B^{1/2}$, one can increase the Landau level mixing either by increasing m^* or by decreasing the magnetic field†. Figure 9 shows the spin-polarized and spin-reversed energy gaps as a function of r_s for a system of 20 electrons [65, 66]. The crossover magnetic field, B_c, below which the spin-reversed excitations are energetically favoured, is $B_c = \left(\Delta_{sp} - \Delta_{sr}\right)/g\mu_B$, where Δ_{sr} (Δ_{sp}) is the spin-reversed (spin polarized) eneregy gap. For GaAs, $B_c \approx 14\,\mathrm{T}$ for $r_s = 2$, and for $r_s = 10$, $B_c \approx 7\,\mathrm{T}$. In fact, figure 9 shows that the Landau level mixing has a weaker effect on Δ_{sr} but has a strong effect on Δ_{sp}. Interestingly, when one includes the finite-thickness correction, B_c is only weakly dependent on the Landau level mixing, and our original results [57, 58] remain valid. This is seen in figure 10 where the energy gaps are plotted with the finite-thickness corrections included.

2.4. *Excitation spectrum*

The excitation spectrum at the FQHE filling factors were calculated by various authors [16, 67, 68] following the recipe of Haldane [16, 67, 69, 70] for a few electrons in a periodic rectangular geometry. The method is described very briefly as follows‡: for every lattice vector $\mathbf{L}_{mn}$, $[ma\hat{\mathbf{x}} + nb\hat{\mathbf{y}}]$, there is a translation operator which commutes with the Hamiltonian. The eigenvalues of this operator are $\exp[2\pi i(ms + nt)/n_d]$, where n_d is the highest common divisor of n_e and n_s. The quantum numbers s and t $(s,t = 0,1,\ldots,n_d - 1)$ are related to the physical momentum by

† For parameters appropriate to GaAs heterostructures, i.e. $\epsilon = 12.6$ and the effective mass $m^* = 0.067m_0$, $r_s = 6.3/[B(\mathrm{tesla})]^{1/2}$.

‡ For details of the formalism see Reference [16].

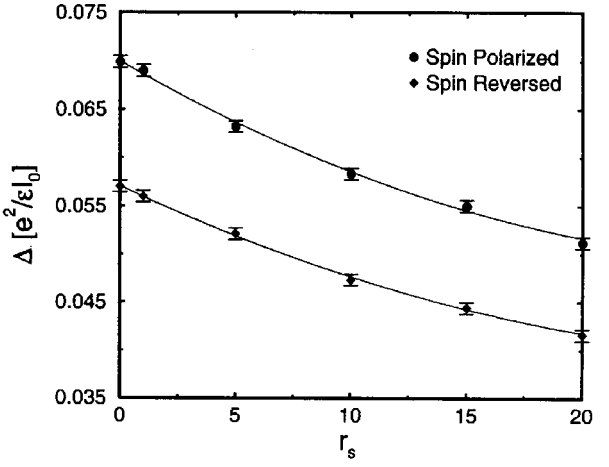

Figure 10. Same as in figure 9, but with finite-thickness correction included [65, 66].

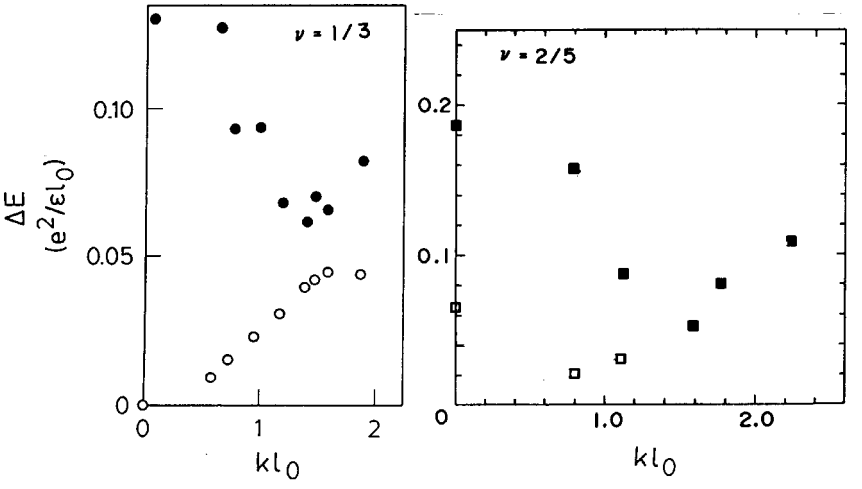

Figure 11. $\nu = \frac{1}{3}$: density-wave spectrum (closed circles) and the spin-wave spectrum (open circles) for a five-electron system. $\nu = \frac{2}{5}$: density-wave spectrum (closed squares) and the spin-wave spectrum (closed squares) for a four-electron system [68].

$$k\ell_0 = \left[\frac{2\pi}{n_s\lambda}\right]^{1/2} [s - s_0, \lambda(t - t_0)],$$

where the point (s_0, t_0), corresponding to the state $\mathbf{k} = 0$, is required to be the most symmetric point of the reciprocal lattice, and $\lambda = a/b$ is the aspect ratio. Using this approach, Yoshioka calculated the density-wave and spin-wave spectra for $\nu = \frac{1}{3}$ and $\nu = \frac{2}{5}$ [68]. The ground state was found at $\mathbf{k} = 0$ for both $\nu = \frac{1}{3}$ and $\nu = \frac{2}{5}$ and, as expected, the total spin of the ground state is $n_e/2$ for $\nu = \frac{1}{3}$ and zero at $\nu = \frac{2}{5}$. The excited states were classified by their values of $|S|$ and S_z. At $\nu = \frac{1}{3}$, the density-wave mode corresponds to the excited states with $|S| = S_z = n_e/2$ and the spin-wave mode corresponds to the excited states with $|S| = S_z = n_e/2 - 1$. The results are shown in figure 11, for zero finite-thickness correction. Clearly, the spin wave mode has almost always lower energies than that for the density-wave mode.

The analysis of the excitation spectrum at $\nu = \frac{2}{5}$ is somewhat complicated. First, it should be noted that the momentum $\mathbf{k}$ is defined modulo $\mathbf{G} = \left(n_1 b/q\ell_0^2, n_2 a/q\ell_0^2\right)$, where n_1 and n_2 are integers and q is the denominator of the filling factor $\nu = p/q$ [16, 67]. However, the density operator

$$\rho_\sigma(\mathbf{k}) = \sum_j \exp\left[-\mathrm{i}\frac{2\pi\ell_0^2}{b}k_x\left(j + \frac{n_s\ell_0^2}{2a}k_y\right) - \frac{1}{4}k^2\ell_0^2\right] a^\dagger_{j+n_s\ell_0^2 k_y/a,\sigma} a_{j,\sigma}$$

is defined as modulo $\mathbf{G}_d = \left(n_1 b/\ell_0^2, n_2 a/\ell_0^2\right)$, which is larger than $\mathbf{G}$ by a factor of q [68]. Therefore, it is possible that the excited states with $\mathbf{k}$ can be a density or spin wave mode with momentum $\mathbf{k} + \mathbf{G}$ in the first *Brillouin zone* of $\mathbf{G}_d$. The other point is that, although the spin wave mode has $|S| = 1$, not all states with $|S| = 0$ belong to the density wave mode; it can also correspond to the state where two spin waves are excited. Yoshioka settled this problem by calculating the matrix element of the total density operator or the spin-density operator between the ground state and the excited states. That way, one can assign the lowest energy density wave and spin wave mode at each allowed value of $\mathbf{k} + \mathbf{G}$ [68]. The results are displayed in figure 11.

2.5. *Tilted-field effects*

Measurement of the FQHE in a tilted field has now become an established technique for investigating spin polarizations at various filling factors. The technique was first applied by Fang and Stiles [71] to study the g factors in Si inversion layers, where they realized that the Landau level spacing $\hbar\omega_c$ depends on the perpendicular component of the field $B_\perp$, but the Zeeman energy depends on the total field B_{tot}. Therefore, by tilting the sample they could vary the two energies independently.

An interesting effect of the tilted field is to make the electron wave function more two dimensional, that is, the tilt angle squeezes the wave function in the z direction. It has been demonstrated in [72] that at a fixed value of the perpendicular component of the magnetic field $B_\perp$, increasing the tilt angle increases the finite-thickness parameter d (introduced in equation (7)) and decreases the dimensionless parameter† $\beta = (d\ell_\perp)^{-1}$. Consequently, the energy gap increases with increasing tilt angle. The electron–hole symmetry for the spin polarized system is, however, not broken by this effect. Early results on the FQHE in a tilted field [73] were explained as a manifestation of this effect.

Another effect of the tilted field is the subband Landau-level coupling, known from the investigations of the single-electron problem [74, 75] and in the FQHE regime [76]. We consider the situation where electrons are confined in the xy plane by a parabolic potential well $V(z) = \mathcal{A}z^2$. This choice of the potential is particularly useful because in this case exact results are available for the single-particle Schrödinger equation [74]. Parameters of the potential are, however, adjusted such that they correspond to the subband energy of a more realistic triangular potential using the Fang–Howard choice of the trial wave function [16]. A magnetic field is applied in the xz plane and we consider the electrons to be in the lowest Landau level and also in the lowest subband. We choose the gauge such that the vector potential is $\mathbf{A} = (0, xB_z - zB_x, 0)$, where $B_x = B\sin\theta$, $B_z = B\cos\theta$ and θ is the tilt angle. The single-particle Schrödinger equation is solved by an appropriate rotation [74] of

† The Coulomb energy is expressed in units of $e^2/\epsilon\ell_\perp$, where $\ell_\perp = (\hbar c/eB_z)^{1/2}$ is the perpendicular component of the magnetic length ℓ_0.

coordinates and the energy eigenvalues are those for two harmonic oscillators with frequencies

$$\omega_{1,2} = \{\tfrac{1}{2}(\omega_c^2 + \omega_0^2) \pm \tfrac{1}{2}[\omega_c^4 + \omega_0^4 + 2\omega_0^2(\omega_x^2 - \omega_z^2)]^{1/2}\}^{1/2}, \tag{11}$$

where $\omega_0 = (2\mathcal{A}/m^*)^{1/2}$, $\omega_z = \omega_c \sin\theta$, $\omega_z = \omega_c \cos\theta$ and m^* is the effective mass. Note that the Landau-level degeneracy and the filling factor depend *only* on the magnetic field component normal to the electron plane.

The Coulomb interaction energy of the electron system subjected to a tilted magnetic field has been evaluated for electrons in a periodic rectangular geometry [16, 76]. The appropriate single-electron states are (compare with equation (5))

$$\varphi_j(\mathbf{r}) = \left(\frac{1}{b\ell_1\ell_2\pi}\right)^{1/2} \sum_{k=-\infty}^{\infty} \exp\{ik_y y/\ell_0^2 - [(k_y - x)\cos\phi + z\sin\phi]^2/2\ell_1^2 - [(k_y - x)\sin\phi - z\cos\phi]^2/2\ell_2^2\}, \tag{12}$$

where a and b are the two sides of the rectangular cell. The magnetic length is $\ell_0 = (\hbar/m^*\omega_z)^{1/2}$ and $\ell_1 = (\hbar/m^*\omega_1)^{1/2}$, $\ell_2 = (\hbar/m^*\omega_2)^{1/2}$. Also, in equation (12)

$$\phi = \tfrac{1}{2}\arctan\left[\frac{\sin(2\theta)}{\cos(2\theta) - \mathcal{A}(2m^*/e^2)}\right] \tag{13}$$

is the angle of rotation of the coordinates to separate the variables in the single-particle Schrödinger equation. The two-electron term of the Hamiltonian is now modified as (compare with equation (6))

$$\begin{aligned} A_{j_1,j_2,j_3,j_4} &= \tfrac{1}{2}\int d\mathbf{r}_1 \int d\mathbf{r}_2 \varphi_{j_1}^*(\mathbf{r}_1)\varphi_{j_2}^*(\mathbf{r}_2) v(\mathbf{r}_1 - \mathbf{r}_2)\varphi_{j_3}(\mathbf{r}_2)\varphi_{j_4}(\mathbf{r}_1) \\ &= \frac{1}{2ab}\sum_{\mathbf{q}}\sum_s\sum_t \delta_{q_x,2\pi s/a}\delta_{q_y,2\pi t/b}\delta'_{j_1-j_4,t}\frac{2\pi e^2}{\epsilon q} \\ &\quad \times \exp[2\pi i s(j_1 - j_3)/n_s - \pi(s^2 + \lambda^2\Omega_1^2 t^2)/(n_s\lambda\Omega_1)]\frac{2}{\pi^{1/2}}\mathcal{I}(s,t)\delta'_{j_1+j_2,j_3+j_4}, \end{aligned} \tag{14}$$

where $v(\mathbf{r})$ is the Coulomb interaction in the periodic rectangular geometry and the Kronecker delta with a prime means that the equality is defined as modulo n_s. The summation over q excludes $q_x = q_y = 0$. The last term in equation (14) is written explicitly as

$$\mathcal{I}(s,t) = \int_0^\infty \exp\left\{-z^2 - 2\left[\frac{\pi}{n_s\lambda}\frac{s^2 + \lambda^2 t^2}{\Omega_3 - \Omega_2^2/\Omega_1}\right]^{1/2} z\right\} \cos\left[2\left(\frac{\pi}{n_s\lambda}\frac{1}{\Omega_3 - \Omega_2^2/\Omega_1}\right)^{1/2}\frac{\Omega_2}{\Omega_1}sz\right] dz \tag{15}$$

and

$$\Omega_1 = \frac{\omega_1}{\omega_z}\cos^2\phi + \frac{\omega_2}{\omega_z}\sin^2\phi,$$

$$\Omega_2 = \left[\frac{\omega_2}{\omega_z} - \frac{\omega_1}{\omega_z}\right]\sin\phi\cos\phi,$$

$$\Omega_3 = \frac{\omega_1}{\omega_z}\sin^2\phi + \frac{\omega_2}{\omega_z}\cos^2\phi. \tag{16}$$

Here λ denotes the aspect ratio. It is easy to check that when $\theta = 0$ and the strength of the confinement potential goes to infinity, i.e. $\omega_0 \to \infty$, we get $\phi = 0$, $\Omega_1 \to 1$, $\Omega_2 \to 0$ and $\Omega_3 \to \infty$. In that limit, equation (14) gives the usual result for a 2DEG with a perpendicular magnetic field.

When the magnetic field is perpendicular to the electron plane there is, of course, electron–hole symmetry in the lowest Landau level. In that case the Hamiltonian does not have any explicit dependence on the magnetic field and in units of potential energy, properties of $\frac{1}{3}$ and $\frac{2}{3}$ filling factors are always the same. In the present case, such an *ideal* situation does not exist, and in order to study angular dependence of the energy gap for $\frac{1}{3}$ and $\frac{2}{3}$, we need to consider the different frequencies which appear in equation (11) for the two filling factors (see equations (14)–(16)). This is a direct consequence of a tilted field. Coupling of subband and Landau levels is found to break the electron–hole symmetry in such a way that the angular dependence of the $\frac{2}{3}$ energy gap rises rapidly, but the gap for the $\frac{1}{3}$ state is almost flat as the tilt angle is increased [76]. The major effect of the tilted field, which is exhibited by various spin transitions in the experiments described below, is to alter the Zeeman energy.

2.6. *Tilted-field experiments: the evidence*

Investigations of the FQHE in tilted magnetic fields began in earnest with the first reported work of Haug *et al.* [77]. They pointed out that in a tilted magnetic field the electron–hole symmetry between the $\nu = \frac{1}{3}$ and $\nu = \frac{2}{3}$ states is broken. Activation energy for the $\frac{1}{3}$-filled state determined from measured temperature dependence of the diagonal resistivity was found to decrease slightly as the tilt angle was increased (the activation energy was found to be $W = 1.67\,\mathrm{K}$ at $\theta = 0^\circ$ and $W = 1.52\,\mathrm{K}$ at $\theta = 63.7^\circ$). On the other hand, for the $\frac{2}{3}$ filling factor, activation energy showed a rapid increase with increasing tilt angle. This observed difference in behaviour between the two filling factors could not be explained by a change of the z extension of the wave function.

2.6.1. *Spin states at $\nu = \frac{1}{3}$ and $\nu = \frac{5}{3}$*

Clark *et al.* [78, 79] probed spin configurations of several fractional states, for the first time, by tilting the field B at an angle θ to the sample plane normal (increasing its absolute value at fixed density n and the perpendicular component $B_\perp$), and also by increasing the density of the system (at $\theta = 0^\circ$) so that the fraction occurs at higher $B_\perp$. They found that, with increasing tilt-angle, dramatic changes occur in the ρ_{xx} minima of various filling factors. In figure 12 we present some of the experimental results of ρ_{xx} versus θ by Clark *et al.* Clearly, the $\frac{4}{3}$ state is first destroyed, followed by a re-emergence as θ and hence the magnetic field is increased. The same effect was also observed for $\nu = \frac{2}{3}$. In contrast, the ρ_{xx} minima for $\frac{5}{3}$ and $\frac{1}{3}$ remain essentially unaltered with increasing tilt angle. In fact, the theoretical work discussed above predict that at low fields, the $\frac{2}{3}$ and $\frac{4}{3}$ states should be spin-unpolarized ($S = 0$).

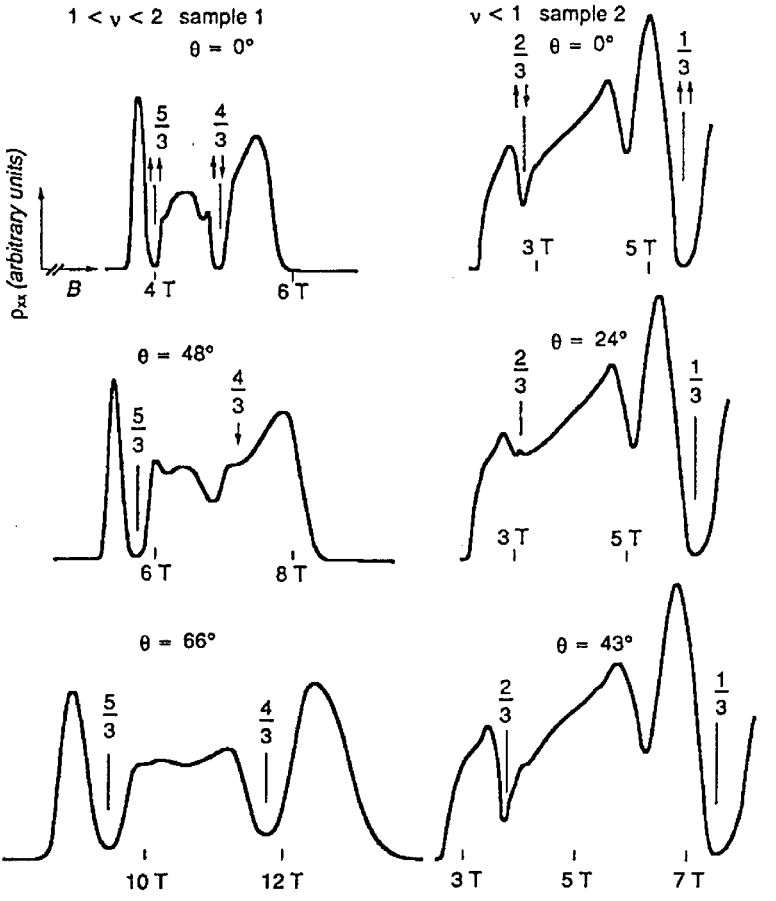

Figure 12. The effect of tilted field on the diagonal resistivity ρ_{xx} for various filling factors versus the magnetic field [78].

An important clue to understanding the experimental results by Clark *et al.* is the fact that, allowing for the spin degree of freedom, the electron–hole symmetry is between ν and $2-\nu$ [38] as discussed in section 2.2. Therefore, the $\frac{1}{3}$ and $\frac{5}{3}$ filling factors which are the spin-polarized states even at low magnetic fields, as predicted theoretically, remain unaffected by the tilted-field. For the $\frac{2}{3}$ and $\frac{4}{3}$ states, the increasing magnetic field destroys the reversed-spin states and eventually, they re-emerge as fully spin-polarized states.

To check that the tilted field is *not* affecting the wave function in the z direction, as discussed above, Clark *et al.* moved the fractional states $\nu = p/q$ to higher $B_\perp$ at $\theta = 0^\circ$ by increasing the electron concentration using persistent photoexcitation techniques. They observed identical effects [79], which indicates that increasing the field simply influences the spin states of different filling factors. The experimental work by Clark *et al.* is an important step in our understanding of the FQHE; it established the theoretical predictions of spin-reversed states discussed in section 2.2, on a firm footing.

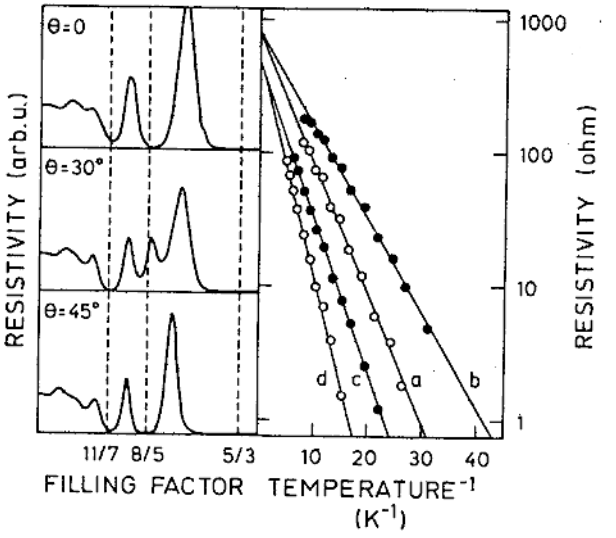

Figure 13. ρ_{xx} versus ν around $\nu = \frac{8}{5}$, exhibiting splitting of the $\frac{8}{5}$ minimum at $\theta = 30^\circ$. Right panel shows the temperature dependence of ρ_{xx} for the $\frac{8}{5}$ minimum at various tilt angles, (*a*) $\theta = 0^\circ$, (*b*) $\theta = 18.6^\circ$, (*c*) $\theta = 42.4^\circ$ and (*d*) $\theta = 49.5^\circ$ [80].

2.6.2. *Spin transitions at* $\nu = \frac{8}{5}$

In the absence of any Landau level mixing, $\nu = \frac{8}{5}$ is electron–hole symmetric to $\nu = \frac{2}{5}$. In this state, Eisenstein *et al.* [80] observed interesting *re-entrant* behaviour in the presence of a tilted magnetic field. When the sample is tilted, the $\frac{8}{5}$ state initially becomes weak (figure 13). Increasing the angle to about $\theta = 30^\circ$, the FQHE minimum splits into two minima of comparable strength whose field positions straddle the location of $\nu = \frac{8}{5}$. In fact, precisely at $\nu = \frac{8}{5}$ the resistivity exhibits a local *maximum*. A further increase of the tilt angle reverses the trend: the high-field component of the doublet becomes dominant and gradually moves on to $\nu = \frac{8}{5}$. For $\theta > 37^\circ$, there is only a single minimum at $\nu = \frac{8}{5}$ which grows stronger as the tilt angle is increased. The Hall resistance shows a plateau at $\rho_{xy} = 5h/8e^2$ in both the low- and high-angle regimes.

Eisenstein *et al.* [80] interpreted these results as due to a phase transition from an unpolarized ground state at small tilt angles to a fully polarized ground state at large tilt angles. This interpretation gains more weight when one looks at the energy gap of $\nu = \frac{8}{5}$, determined from the activated temperature dependence of the resistivity. The resulting energy gap Δ is plotted in figure 14 as a function of the *total* magnetic field $B_{\rm tot}$, where the perpendicular component of the field is fixed at $B_\perp = 5.95$ tesla. As seen in the figure, the energy gap decreases *linearly* with $B_{\rm tot}$ at small tilt angles and rises linearly with $B_{\rm tot}$ in the high-angle regime. The magnitudes of the slopes $|\partial\Delta/\partial B_{\rm tot}|$ are nearly equal in the two phases, and a g factor deduced from the slope is $\sim$0.4, close to the bulk GaAs value. These facts led the authors to interpret the results as a spin transition where for $B_{\rm tot} < 7$ T (i.e. $\theta < 30^\circ$), the system corresponds to an unpolarized ground state with $\Delta S = +1$, where ΔS is the difference in spin of the quantum liquid state before and after the excitation of a quasiparticle–quasihole pair [80]. For $B_{\rm tot} > 7$ T, the ground state is spin polarized but $\Delta S = -1$. We wish to point out the striking resemblance between the observed energy gap and what we predicted theoretically at $\nu = \frac{2}{5}$ (see figure 6 (*a*)).

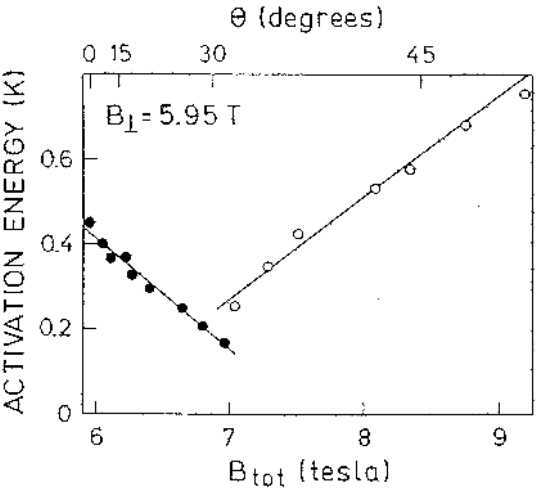

Figure 14. Energy gap Δ of $\nu = \frac{8}{5}$ as a function of the total magnetic field B_{tot} [80].

2.6.3. *Spin transitions at* $\nu = \frac{2}{3}$ *and* $\nu = \frac{4}{3}$

The energy gap at $\nu = \frac{2}{3}$ and signatures of possible spin transitions on the magnetic-field dependence of the energy gap was studied by several authors. As discussed above, experimental results of Haug *et al.* [77] with tilted magnetic fields indicated an apparent violation of the electron–hole symmetry between $\nu = \frac{1}{3}$ and $\frac{2}{3}$ with fully spin-polarized ground states and excitations. Eisenstein *et al.* [81] observed a re-entrant behaviour at $\nu = \frac{2}{3}$ and explained it as being most likely the result of spin transitions. Clark *et al.* [82] found that in a tilted-field experiment and at a fixed temperature T, the depth of the ρ_{xx} minimum at $\nu = \frac{2}{3}$ was reduced over a range of tilt angle which would most likely indicate a minimum in the energy gap as a function of the total magnetic field. They also observed a splitting of the ρ_{xx} minimum at $\frac{2}{3}$ at angles where the minimum was weakest. Eisenstein *et al.*, however, did not observe any such splitting. They also did not observe any linear region of the energy gap at $\nu = \frac{2}{3}$.

Engel *et al.* [83] studied the gap at $\nu = \frac{2}{3}$ and $\nu = \frac{3}{5}$ in a tilted magnetic field. They found that at both these filling factors the energy gap Δ versus the total magnetic field B_{total} exhibited minima which were accompanied in transport by splitting of the ρ_{xx} minimum. The result for the activated energy gap Δ (K) versus the total magnetic field B_{total} obtained by Engel *et al.* is displayed in figure 15. They observed a prominent minimum at a critical field of $B_{\text{c,total}} = 1.83 \pm 0.02$ T. For a magnetic field well above this critical field ($B_{\text{total}} > 2.1$ T), the data for Δ is fit very well by a straight line of slope $0.4\mu_{\text{B}} \approx g\mu_{\text{B}}$ for GaAs, indicating the Zeeman energy contribution corresponding to a single spin flip. The splitting of the FQHE, which depends on the tilt angle and the minimum in the gap versus B_{total}, were explained by these authors as being the result of ground-state spin transitions, as predicted in the theoretical work discussed above. They did not, however, observe any region in B_{total} where the gap completely vanishes, in contrast to the expectations from the theorteical work at $\nu = \frac{2}{3}$ described above. Of course, it is noteworthy that these experimental results at $\nu = \frac{2}{3}$ are different from those at $\nu = \frac{8}{5}$ because in the present case there are no sharp transitions present in the energy gap as a function of magnetic field. Instead, the

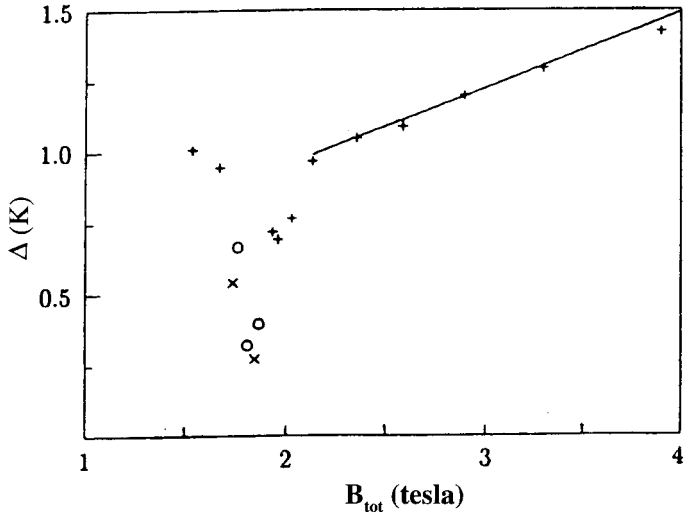

Figure 15. The activation energy gap versus the total magnetic field at $\nu = \frac{2}{3}$ [83].

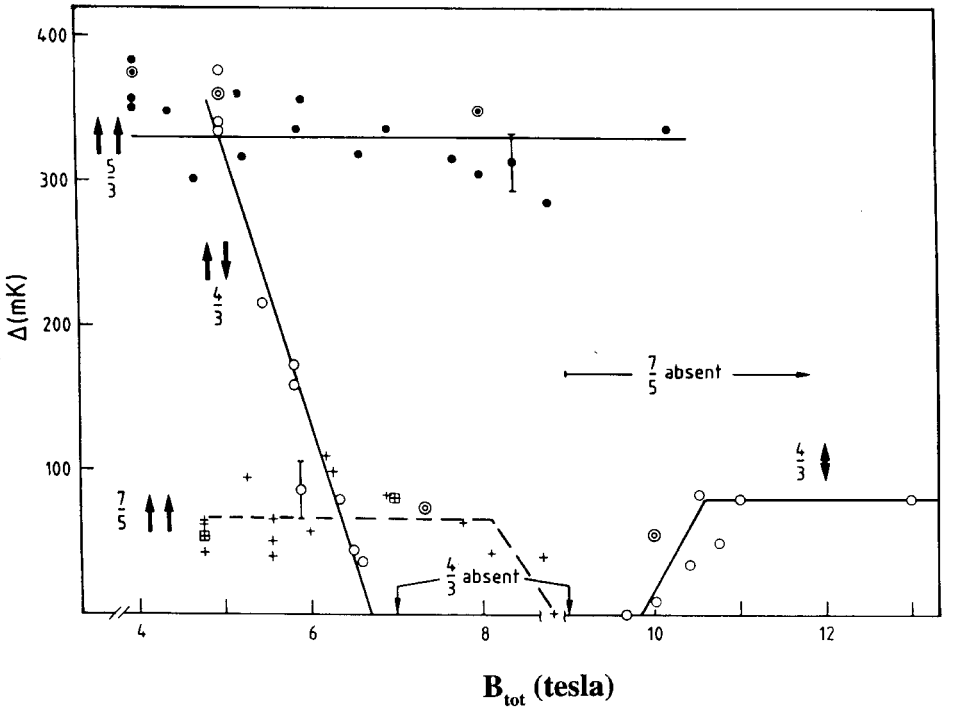

Figure 16. Activation energy gap at $\nu = \frac{4}{3}, \frac{5}{3}$ and $\nu = \frac{7}{5}$ versus the total magnetic field [79].

energy gap at $\nu = \frac{2}{3}$ does show a sharp drop, very near $B_{c,total}$ and exhibits a *linear* increase in both directions away from $B_{c,total}$.

The activation energy gap, measured by Clark *et al.* [79] for $\nu = \frac{4}{3}, \frac{5}{3}$ and $\frac{7}{5}$ versus the total magnetic field, are displayed in figure 16. The disparity between the $\frac{4}{3}$ and $\frac{5}{3}$ states is quite striking: while $\Delta_{5/3}$ remains virtually unchanged over the entire range

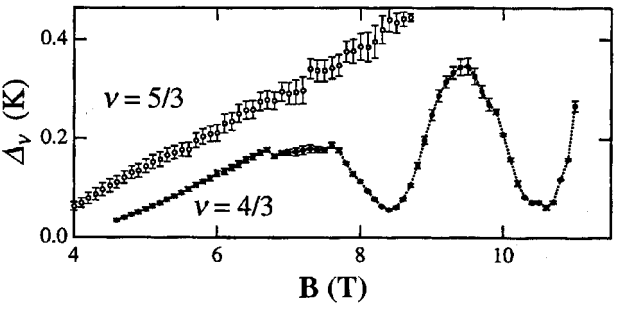

Figure 17. Activation energy gap at $\nu = \frac{4}{3}$ and $\frac{5}{3}$ as a function of the magnetic field [44].

of magnetic field studied, $\Delta_{4/3}$ collapses from 340 mK at $\theta = 0^\circ$ ($B_\perp = 5$ T) to zero over the range $B = 5$–6.7 T. The $\frac{4}{3}$ state is absent in the magnetic field range of $B = 7$–9 T and reappears at higher magnetic fields.

Sachrajda *et al.* [84] reported activation measurements on $\nu = \frac{2}{3}, \frac{4}{3}, \frac{5}{3}$ and $\frac{7}{5}$ as a function of carrier density. The results are consistent with the observations of Clark *et al.* [78] and support the picture of spin polarizations at these filling factors. Tilted field activation measurements at $\nu = \frac{5}{3}, \frac{4}{3}$ and $\frac{7}{5}$ as a function of carrier density were also reported by this group [85]. At $\nu = \frac{4}{3}$ and $\frac{7}{5}$, a strong density dependence was observed. Linear behaviour of the activation gap at $\nu = \frac{2}{3}$ was also reported in [86].

Supporting evidence to the results of Clark *et al.* [78] also came from Davies *et al.* [40] who reported very interesting FQHE experiments in high-quality p-type heterojunctions with tilted magnetic field. They found the same magnetic-field dependent behaviour for $\nu = \frac{4}{3}$ as observed in n-type heterojunctions by Clark *et al.* They also noted that for the two-dimensional hole system one requires a smaller magnetic field to destroy and return the $\frac{4}{3}$ state which suggests that the Zeeman splitting is larger for the present system. In the two-dimensional hole system grown in a symmetrically modulation-doped quantum well, remarkable transitions at $\nu = \frac{4}{3}$ and $\nu = \frac{7}{5}$, similar to those observed by Davies *et al.* were also reported in [42] by varying the potential symmetry of the quantum well structure and thereby varying the valence band structure [43].

Muraki and Hirayama observed the re-entrant behaviour for the $\nu = \frac{4}{3}$ FQHE state by varying the density of a 2D hole gas confined in a modulation-doped quantum well [44]. Similar re-entrant behaviour of the $\frac{4}{3}$ FQH state in a high mobility 2D hole system by changing the carrier density, was observed earlier by Rodgers *et al.* [41]. However, the results of Muraki and Hirayama revealed a very unusual behaviour. Here the activation gap $\Delta_{4/3}$ initially increases with magnetic field and then shows two distinct minima at $B = 8.4$ T and $B = 10.4$ T (figure 17). In contrast, $\Delta_{5/3}$ increases steadily over the entire range of the magnetic field. Observation of the two minima of $\Delta_{4/3}$ is yet to be explained. It is difficult to explain this observation owing to LL mixing because such a mixing would break the particle–hole symmetry of the $\frac{5}{3}$ state to the $\frac{1}{3}$ state. In these results, the $\frac{5}{3}$ state seems to be stable over the entire magnetic field range, which is expected from the particle–hole symmetry related to the $\frac{1}{3}$ state. The prominent oscillation in the $\nu = \frac{4}{3}$ activation energy results must be related to spin transitions at this filling factor which are not present for $\nu = \frac{5}{3}$. The details are, however, need to be worked out.

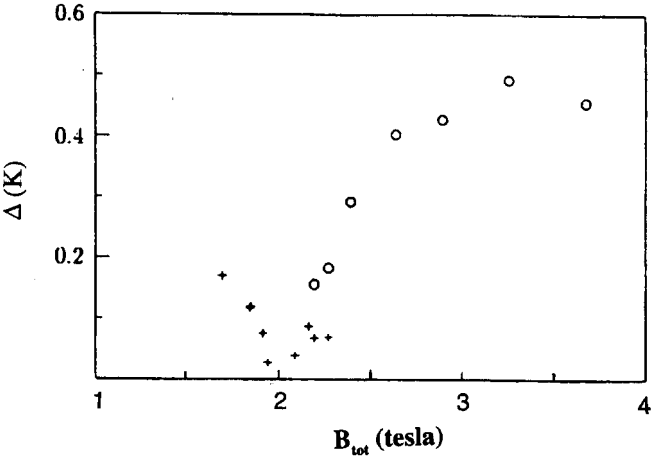

Figure 18. The energy gap versus the total magnetic field at $\nu = \frac{3}{5}$ [83].

2.6.4. *Spin transitions at* $\nu = \frac{3}{5}$ *and* $\nu = \frac{7}{5}$

The results for the activated energy gap versus the total magnetic field at $\nu = \frac{3}{5}$ obtained by Engel *et al.* [83] is displayed in figure 18. As discussed in the theoretical results for this filling factor, the gap structure is much more complicated than that for $\nu = \frac{2}{3}$ or $\frac{2}{5}$. A minimum in the gap is clearly visible and for magnetic fields near the critical field, the energy gap structures qualitatively resemble those of region III, IV and V of figure 8. The energy gap of the $\nu = \frac{7}{5}$ state (electron–hole symmetric to $\nu = \frac{3}{5}$) was measured by Clark *et al.* [79] and is shown in figure 16. These authors noted that, just like the energy gap for the $\frac{4}{3}$ state, the energy gap of this state decreases rapidly and disappears beyond 9 T.

2.7. *Other related experiments*

Kukushkin *et al.* [87, 88] investigated the spin configurations of the QHE states at various filling factors using time-resolved radiative recombination of photoexcited holes bound to acceptors. The $\nu = \frac{2}{3}$ FQHE state was observed to be spin unpolarized (as expected from theoretical investigations) for $B = 1.7$ T, and a fully spin-polarized state for $B > 4$ T. In between these two magnetic field values, there is a gradual transition from the initial spin state (unpolarized) to the final (spin polarized) state. In a more refined experiment, these authors noticed a half-polarized state midway between the spin transitions. This will be discussed in section 3.4.

Although the activation energy measurements provide information about the quasielectron–quasihole gap, the spin polarizations of individual quasiparticles cannot be studied in this method. Dorozhkin *et al.* [89, 90] explored the different spin orientations of quasielectrons and quasiholes via capacitance spectroscopy and magnetotransport. The magnetocapacitance between the 2DES and the gate provides information of the lowest state energy of a 2DES. In a tilted magnetic field, variation of energy with the in-plane component of the magnetic field is used to analyse the spin configurations at $\nu = \frac{1}{3}$ and $\nu = \frac{2}{3}$. The degree of spin polarization was found to be constant at $\nu < \frac{2}{3}$, but decreases at $\nu \geq \frac{2}{3}$. These results are taken as indications for the existence of spin-reversed quasielectrons and spin-polarized quasiholes in agreement with the theoretical predictions [48, 57, 58].

3. Recent developments

After a few relatively quiet years following the tilted-field studies, investigations of the spin-reversed ground state and excitations took off with renewed enthusiasm where new ideas were introduced and more refined experiments were performed. New dimensions were added by looking at the temperature dependence of the spin polarization, as well as the pressure-induced zero Zeeman gap. These results are the topics of the following sections.

3.1. *Temperature dependence: experimental results*

A very ingenious and direct approach to study spin polarizations of a 2DES in the QHE regime using optically-pumped nuclear magnetic resonance (OPNMR) spectra was reported by Barrett *et al.* [91]. They measured the Knight shift $K_s(\nu, T)$ of the ^{71}Ga nuclei located in n-doped GaAs quantum wells using optically pumped nuclear magnetic resonance [92, 93]. For details of those experiments we refer to the original publications [91–93]. Very briefly, the samples consist of forty GaAs quantum wells 300 Å wide and separated by $Al_{0.1}Ga_{0.9}As$ barriers 1800 Å wide. The nuclear spins in the multiple quantum well structure are strongly polarized by optical pumping of interband transitions with near-infrared laser light. Optical pumping generates electrons and holes in the GaAs wells with non-equilibrium spin polarizations, which in turn polarize the nuclei in the well through electron–nucleus hyperfine couplings. From the radio-frequency measurements of ^{71}Ga NMR spectra, Barrett *et al.* studied the shift between the lower frequency, attributed to ^{71}Ga nuclei in the quantum wells, and the higher frequency resonance due to ^{71}Ga nuclei in the barrier. The shift is supposed to have occurred as a result of the magnetic hyperfine coupling between the ^{71}Ga nuclei and electrons in the wells. The hyperfine coupling constant was found to be isotropic in those experiments and therefore the observed NMR frequency shift is a direct measure of the electron spin polarization. These studies include the integer [91] and fractional [94] QHE regime.

Temperature dependence of the Knight shift for $\nu = 0.98$ and $B = 7.05$ T measured by Barrett *et al.* is shown in figure 19. In this figure, the dashed line

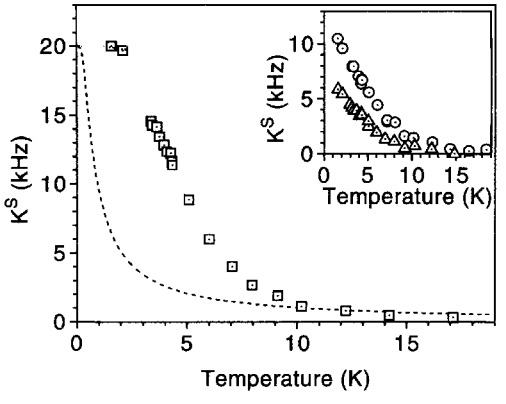

Figure 19. Experimental results for the temperature dependence of the Knight shift for $\nu = 0.98$ and $B = 7.05$ T (open squares). The dashed line is the theoretical result obtained for a non-interacting electron system. The temperature dependence of K_s for $\nu = 0.88$ (open circles) and $\nu = 1.2$ (open triangles) at $B = 7.05$ T is given as an inset [91].

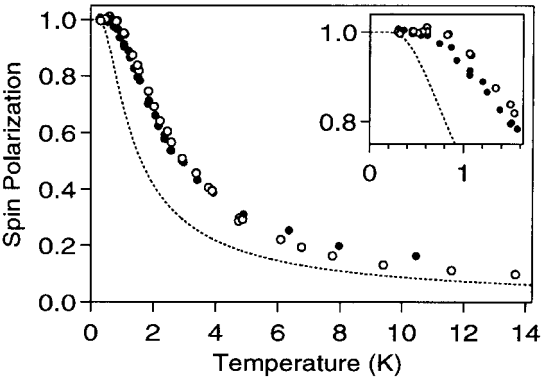

Figure 20. Experimental results for the electron spin polarization as a function of temperature at $\nu = \frac{1}{3}$ [94]. The dashed line is the spin polarization of non-interacting electrons at $\nu = 1$ (see text). The inset depicts the saturation region. The dashed line is the spin polarization of non-interacting electrons for the $\nu = 1$ QHE state (see text).

corresponds to a non-interacting electron system where the chemical potential lies in the middle of the Zeeman gap, $K_s(T) = K_s(0)\tanh(E_z/4k_BT)$, $K_s(0) = 20\,\text{kHz}$ and $E_z/k_B = 2.08\,\text{K}$. Quite clearly, this simple model does not fit the data, notably at low temperatures, where a rapid drop of K_s (and hence a rapid drop in spin polarization) was observed.

In figure 20, we show the temperature dependence of electron spin polarization for $\nu = \frac{1}{3}$, observed by Khandelwal *et al.* [94]. In the figure, for comparison, these authors also plotted the spin polarization of non-interacting electrons at $\nu = 1$, described above, but now with $B = 12\,\text{T}$. They also noted that a value of $\Delta \approx 2E_z$ in $\tanh(\Delta/4k_BT)$ provides a good fit for the saturation region. These experimental results are in excellent agreement with the theoretical results to be discussed below.

The original work of Barrett *et al.* [91] described above prompted other groups to investigate spin polarizations by various other means. Manfra *et al.* [95,96] measured the temperature dependence of spin polarizations at the $\nu = 1$ quantum Hall state using magnetoabsorption spectroscopy which distinguishes the occupancy of the two electron spin states. The results are very similar to those of figure 19.

Investigations by Kukushkin *et al.* [87, 88] of spin polarizations from the analysis of circular polarization of time-resolved radiative recombination of 2D electrons with photoexcited holes bound to acceptors, discussed above, also provide results for the temeparture dependence of spin polarizations. These results for the $\nu = \frac{2}{3}$ FQHE state, measured at different magnetic fields, are shown in figure 21. In the low-field case ($B = 2.12\,\text{T}$), spin polarization reveals a non-monotonic behaviour with increasing temperature, in agreement with the theoretical predictions [97] (see below). At a higher magnetic field ($B = 3.38\,\text{T}$), the decrease of electron spin polarization is more gradual.

3.2. *Temperature dependence: theoretical work*

One important result of the NMR Knight-shift studies of the two-dimensional electron gas is the temperature dependence of $\langle S_z \rangle$. In the canonical ensemble

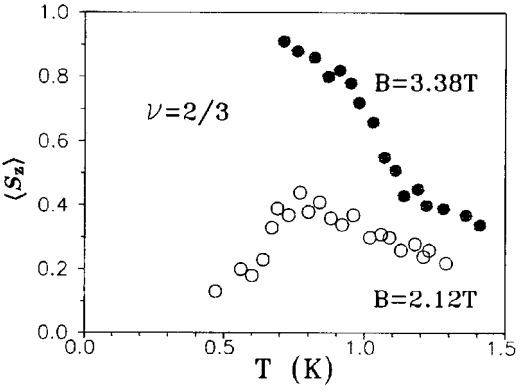

Figure 21. Experimental results for the electron spin polarization as a function of temperature at $\nu = \frac{2}{3}$ for magnetic fields $B = 2.12\,\mathrm{T}$ and $B = 3.38\,\mathrm{T}$ [87].

$$\langle S_z(T)\rangle \equiv \frac{1}{Z}\sum_i \exp(\varepsilon_i/kT)\langle i|S_z|i\rangle,$$

where the summation runs over all states including all possible polarizations

$$\langle i|S_z|i\rangle = -n_e/2,\ldots,0,\ldots,n_e/2,$$

ε_i is the energy of state $|i\rangle$, with Zeeman coupling included, i.e.

$$\varepsilon_i = E_i - g\mu_B B\langle i|S_z|i\rangle,$$

and Z is the canonical partition function

$$Z = \sum_i \exp(-\varepsilon_i/kT).$$

The ground state and the excited states for a given filling factor can be calculated, e.g. from the exact diagonalization of a few-electron system Hamiltonian in a periodic rectangular geometry [16]. In the absence of the Zeeman term in the Hamiltonian $\mathcal{H}$, for each state $|i\rangle$ with $S_z|i\rangle = s_z|i\rangle$ and $\mathcal{H}|i\rangle = \mathcal{E}|i\rangle$, there is a state $|i'\rangle$ for which $\mathcal{H}|i'\rangle = \mathcal{E}|i'\rangle$ but $S_z|i'\rangle = -s_z|i'\rangle$. These terms cancel each other in the sum of $\langle S_z\rangle$. On the other hand, if the Zeeman term is included in the Hamiltonian, $\langle S_z\rangle \neq 0$ because these terms then sum up to [97],

$$s_z \exp(-\beta\mathcal{E})[\exp(\beta g\mu_B s_z B) - \exp(-\beta g\mu_B s_z B)] = 2s_z \exp(-\beta\mathcal{E}) \sinh(\beta g\mu_B s_z B).$$

Generally, the sum over all energy states will then yield a non-vanishing polarization. However, the system can still be unpolarized at $T = 0$ if the ground state, even in the presence of the Zeeman coupling, is unpolarized.

In figure 22, we show the numerical results for $\langle S_z(T)\rangle / \max\langle S_z\rangle$ as a function of T (in units of potential energy†) for the $\nu = \frac{1}{3}$ filling factor. In this calculation the magnetic field value is fixed at 10 T, but a range of g values are considered. We consider a five-electron system in a periodic rectangular geometry. Here the ground state is known to be fully spin polarized, and except for very small values of Zeeman energy where spin-reversed quasiparticles are energetically favourable, the excited

† The conversion factor for T is, e.g. $e^2/\epsilon\ell_0 = 51.67B^{1/2}$ for parameters appropriate to GaAs, where the energy is expressed in K and the magnetic field B is expressed in tesla.

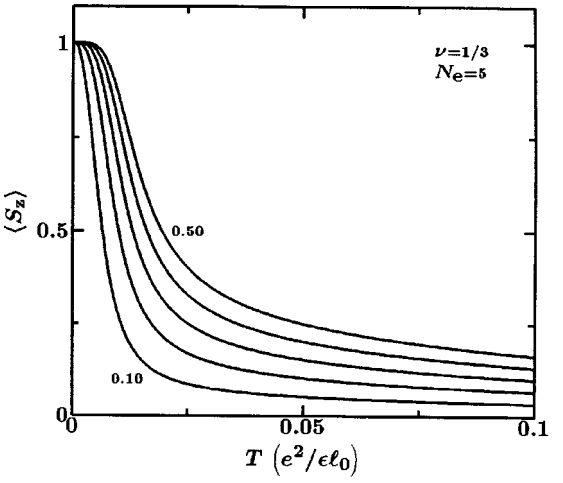

Figure 22. Electron spin polarization $\langle S_z(T)\rangle$ versus the temperature T at $\nu = \frac{1}{3}$ for a magnetic field of 10 T and various values of the g factor.

states are also expected to be spin polarized. This is precisely what is seen at $T = 0$ for even the lowest value of g we consider here.

When the Zeeman energy is decreased (i.e. the g values are reduced), $\langle S_z(T)\rangle$ drops off more rapidly with increasing temperature. For large T, we notice a $1/T$ decay of $\langle S_z(T)\rangle$. This result can be explained by the following arguments: in the limit $T \to \infty$ the leading term in the expansion of $\langle S_z(T)\rangle$ is

$$s_z^{(0)}[1 - \exp(-2\beta g\mu_B s_z^{(0)} B)]$$

when the ground state has non-vanishing polarization $s_z^{(0)}$. If the ground state is unpolarized then the leading term is

$$-2s_z^{(1)} \exp[-\beta(\mathcal{E}_1 - \mathcal{E}_0)] \sinh(\beta g\mu_B s_z^{(1)} B),$$

where $\mathcal{E}_0$ is the energy of the ground state and $\mathcal{E}_1 - g\mu_B s_z^{(1)} B$ the lowest energy with non-vanishing polarization $s_z^{(1)}$. At the high-temperature limit these expressions above are both proportional to B/T. Therefore, at high temperatures the system behaves like a Curie paramagnet [97].

Temperature dependence of $\langle S_z(T)\rangle$ at higher order filling factors show even more interesting features. For example, at $\nu = \frac{2}{3}$ and $\nu = \frac{2}{5}$, we know that the ground states are spin singlets for low Zeeman energies discussed above. At low Zeeman energies, the curves peak at $T \sim 0.01$ (figures 23 and 24) and then at high temperatures they decrease as $1/T$. The appearence of the peak is presumably related to the 're-entrant' behaviour of the activation energy observed earlier in transport measurements and discussed in section 2.6. This behaviour was associated [97] with a phase transition from one spin ground state (unpolarized) to the other (polarized but with spin-reversed excited states) [48, 72, 80]. It is quite likely that, at the low-temperature side of the peak, the system has a spin-reversed ground state as well as spin-reversed excitations. At the high-temperature side of the peak, the system, on the other hand, has a spin-polarized ground state but the excitations are still spin reversed. Theoretical predictions of the temperature dependence of $\langle S_z(T)\rangle$

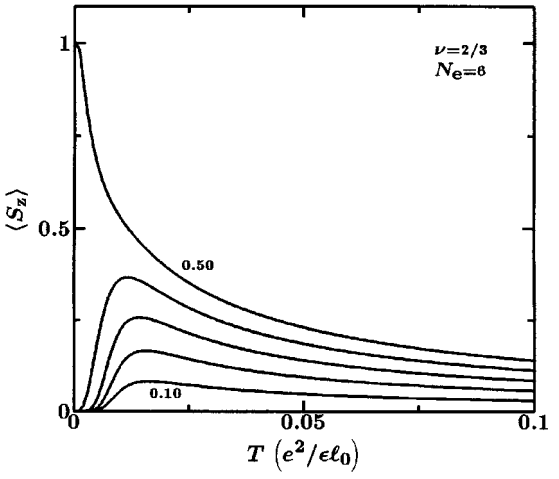

Figure 23. Electron spin polarization $\langle S_z(T)\rangle$ versus the temperature T at $\nu = \frac{2}{3}$ for various values of the g factor.

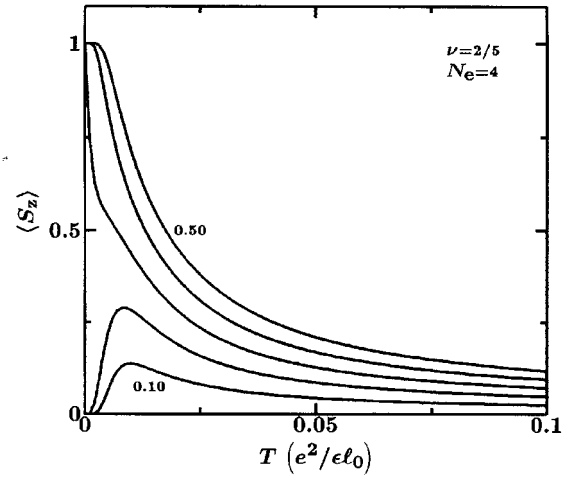

Figure 24. Electron spin polarization $\langle S_z(T)\rangle$ versus the temperature T at $\nu = \frac{2}{5}$ for various values of the g factor.

at $\nu = \frac{2}{3}$ described above (figure 23) are in excellent agreement with the corresponding experimental results discussed above (figure 21).

At $\nu = \frac{3}{5}$, the ground state is at $S = 1$ (and accordingly $S_z = 0$ and $S_z = 1$ are degenerate in the absence of Zeeman coupling). This means that the system will be at least partially polarized no matter what value of g one considers (except for $g = 0$, when, of course, $\langle S_z\rangle = 0$). For low values of g and at low temperatures, we see (figure 25) a gradual formation of the peak in $\langle S_z(T)\rangle$ and a transition to the fully polarized state when g is further increased [97]. This behaviour is consistent with the behaviour of $\langle S_z(T)\rangle$ at other filling fractions discussed above and can be interpreted as transitions from the partially polarized to a spin-singlet state and eventually to a fully polarized state. The high-temperature behaviour is, however, the same as in all other filling fractions described here.

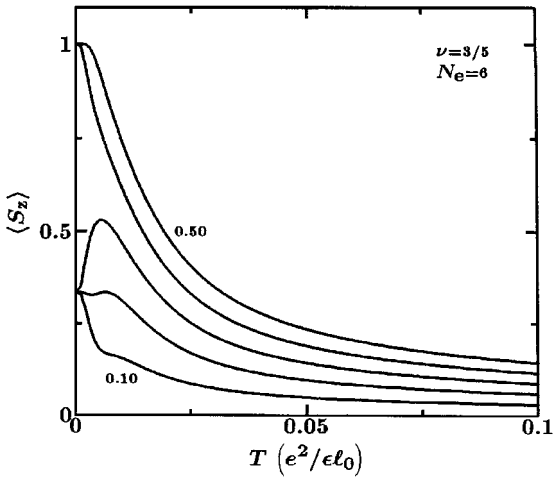

Figure 25. Temperature dependence of the electron spin polarization at $\nu = \frac{3}{5}$ for various values of the g factor.

3.3. *Vanishing Zeeman energy: more evidence*

The possibility of realizing a two-dimensional electron system with a vanishingly small g factor via application of pressure was pointed out earlier in the literature [98]. Application of a hydrostatic pressure is expected to produce changes in the band structure and the spin–orbit coupling, which would result in a reduction in the magnitude of the Landé g factor experienced by the electrons. An enhancement of the FQHE at $\nu = \frac{4}{3}$ with increasing hydrostatic pressure was interpreted as resulting from the pressure-induced reduction of the g factor [98]. This method of changing the Zeeman energy of fractional states seems to be an attractive alternative to the conventional rotation of the sample described above.

3.3.1. *Spin transitions at* $\nu = \frac{2}{5}$

Kang *et al.* [99] studied the spin transitions at $\nu = \frac{2}{5}$. Their experiments involved high mobility GaAs heterostructures subjected to pressures up to 14 kbar. They noticed that with increasing pressure the FQHE states at $\nu = \frac{2}{5}$ (and also $\nu = \frac{3}{7}$) gradually disappear. At pressures slightly above the critical pressure where the state collapses, a re-entrant behaviour at $\nu = \frac{2}{5}$ was induced by rotating the sample relative to the applied magnetic field. As discussed above, these results indicate a transition from a spin-polarized ground state at low pressures to a spin-unpolarized ground state at high pressures. Application of hydrostatic pressure results in a decrease in the magnitude of the g factor which in turn reduces the Zeeman energy and drives the spin transition.

The energy gap of the FQHE state at $\nu = \frac{2}{5}$, obtained by Kang *et al.* [99] at different magnetic fields is shown in figure 26. Each data point corresponds to a different pressure and therefore corresponds to a different g value. The energy gap at the highest and lowest magnetic fields shown here correspond to 11.2 and 14.2 kbar of pressure, respectively. A minimum in the energy gap at around 8 T of magnetic field corresponds to 13.8 kbar of pressure. These authors estimated that the $\nu = \frac{2}{5}$ state is spin polarized below 13.5 kbar of pressure and spin unpolarized at higher pressures.

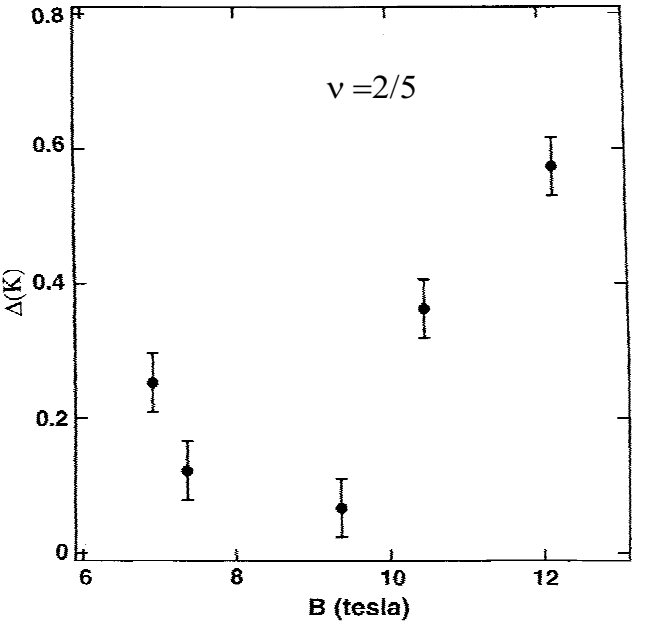

Figure 26. Energy gap at $\nu = \frac{2}{5}$ [99]. Each datum point corresponds to different pressures (see text).

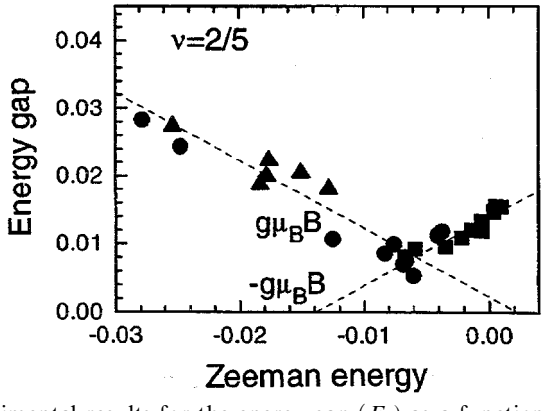

Figure 27. Experimental results for the energy gap (E_g) as a function of the Zeeman energy (E_z) at $\nu = \frac{2}{5}$ [100].

In the experimental study of Leadley *et al.* [100], hydrostatic pressure of up to 22 kbar was applied to the sample. In GaAs, application of a hydrostatic pressure reduces the magnitude of g from 0.44 which approaches zero at ~ 18 kbar. They also observed a re-entrant behaviour of the activation energy gap at $\nu = \frac{2}{5}$ which, as discussed above, indicates that a spin transition from the unpolarized to a fully spin polarized spin state has taken place at that filling factor (figure 27).

There is a clear correspondence between the results of these two groups and the re-entrant behaviour at $\nu = \frac{8}{5}$ observed earlier in magnetotransport experiments, as discussed above. From these results it can be safely concluded that the spin properties of $\nu = \frac{2}{5}$ and its electron–hole conjugate, $\nu = \frac{8}{5}$ predicted in the theoretical studies [16, 20, 32, 35] in low magnetic fields is now well established.

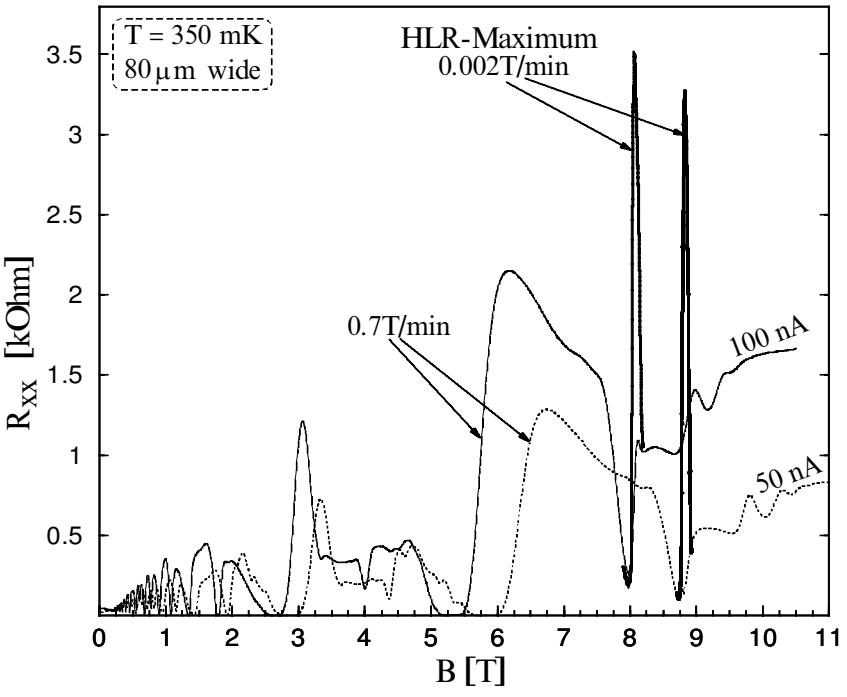

Figure 28. Longitudinal resistance at 0.4 K and for two different electron densities. The 'slow' sweep corresponds to 0.002 T min^{-1}, and the 'fast' sweep rate is 0.7 T min^{-1} [101,103].

3.4. *Hysteresis and spin transitions*

Our predictions of the nature of spin polarizations and magnetic field dependence at $\nu = \frac{2}{3}, \frac{3}{5}$ and $\nu = \frac{2}{5}$ (figures 3, 6, 7 and 8) has received strong support from two very interesting recent experiments at these filling factors [101, 102]. Kronmüller *et al.* [101] used high mobility and *narrow* quantum well (15 nm thickness and 120 nm spacer thickness) structures and the samples were processed as Hall bars of two different widths (80 and 800 μm). For the 80 μm Hall bar at 0.4 K, a (standard) sweep rate of 0.7 T min^{-1} and a current of 100 nA did not produce any unusual behaviour in the longitudinal resistance R_{xx}. In the fractional regime, the minimum of R_{xx} was found to approach zero at $\nu = \frac{2}{3}$. However, at a much slower sweep rate (0.002 T min^{-1}), a large and sharp ($\Delta B \approx 0.2$ tesla) *maximum* appeared very close to $\nu = \frac{2}{3}$ (figure 28). Clearly, this peak stands out over all the other maxima in the surrounding magnetic field region: the peak value of R_{xx} exceeds those of the surrounding values by up to a factor of three. Even when the carrier density was varied over the range 1.2×10^{15} to 1.4×10^{15} m^{-2} the position of the maximum remained at $\nu = \frac{2}{3}$. The formation of the huge longitudinal resistance maximum (HLRM) takes place on a very large time scale. Typically, for a 80 μm wide Hall bar it takes 10 min for the maximum to saturate, while it takes 50 min for the 800 μm bar. At lower temperatures, a similar maximum was also observed at $\nu = \frac{3}{5}$ (figure 29).

Given the significant time and size dependence of the HLRM it is not surprising that the HLRM exhibits hysteretic effects (figure 30). For an up-sweep of the magnetic field, the position of the maximum is at slightly higher fields. On the other

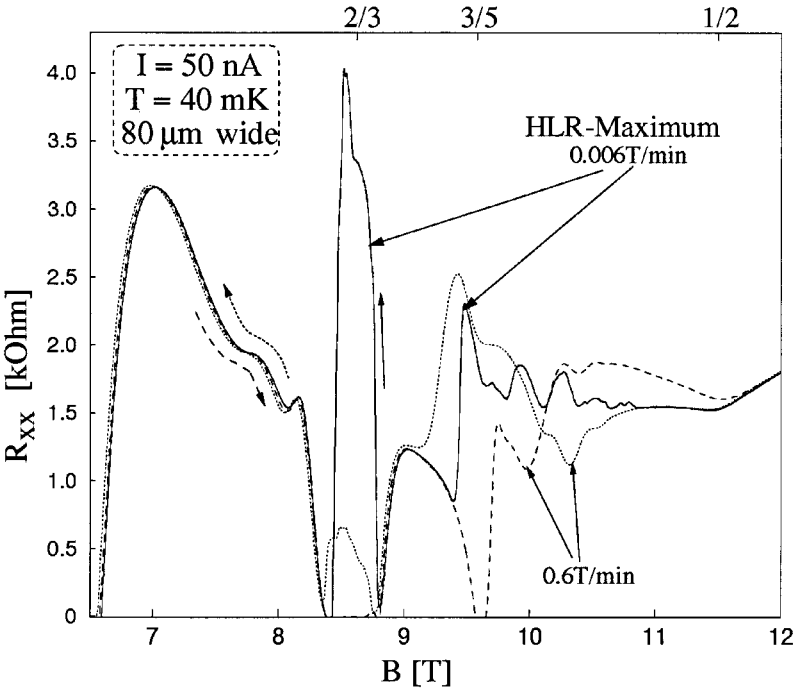

Figure 29. Longitudinal resistance at 40 mK. The dashed curve corresponds to 'up-sweep' at $0.6\,\mathrm{T\,min^{-1}}$. The dotted curve is for 'down-sweep' at $0.6\,\mathrm{T\,min^{-1}}$ and the solid line is for slow down-sweep ($0.006\,\mathrm{T\,min^{-1}}$) [101,103].

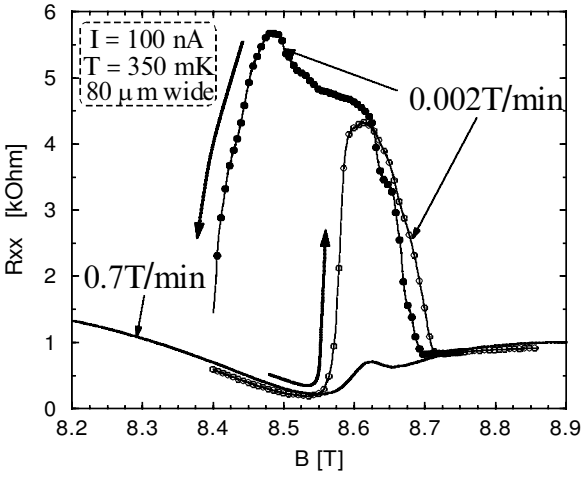

Figure 30. Observed hysteresis of the HLRM at 0.4 K [103].

hand, for a down sweep, the maximum is much wider and more symmetric around $\nu = \frac{2}{3}$.

These surprising observations have been attributed to the fact that the electronic system spontaneously separates into different domains, and scattering of the charge carriers off the domain walls contribute to the high resistance. If the experimental

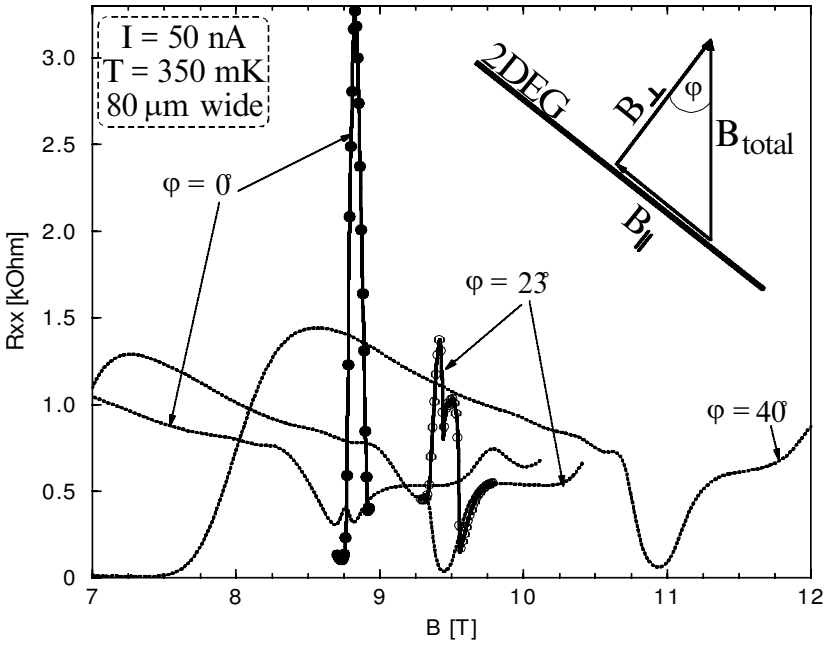

Figure 31. Longitudinal resistance for different tilt angles. Results for the fast sweep are shown as broken lines, and solid lines correspond to slow sweep. At 40°, the effect is no longer visible for sweep rates down to $0.002\,\mathrm{T\,min^{-1}}$ [103].

situation happens to be where the ground state energies of the two different spin states are nearly degenerate (figures 3(*b*) and 7) such a domain structure is entirely conceivable. No such competing states are predicted at $\nu = \frac{1}{3}$ or other nearby filling factors in these experiments and no maximum was observed at any other filling factors. The fact that these observations were related to the spin properties was underscored in tilted field measurements where the maxima were found to disappear completely at tilt angle of 40° (figure 31).

Cho *et al.* [102] observed hysteretic behaviour at $\nu = \frac{2}{5}$ under hydrostatic pressure, which, as described in section 3.3, seems to be an essential ingredient for inducing a spin transition at this filling factor. They observed indications of similar hysteretic behaviour also at $\nu = \frac{4}{7}$ and $\frac{4}{9}$. Since hysteresis often accompanies a first-order phase transition, these authors concluded that the transition between FQHE liquids with different spin polarizations is perhaps a first-order phase transition. It is fairly obvious that the threshold magnetic field (or the *g* factor) for a spin transition strongly depends upon the filling factor. While the transitions are observed at higher *g* values at $\nu = \frac{2}{3}$, hydrostatic pressure is essential to reduce the *g* factor in order to observe the spin transition at $\nu = \frac{2}{5}$. This is quite apparent in our theoretical results shown in figures 23 and 24.

As mentioned above, the HLRM develops within a time period of the order of minutes and hours, depending upon the width of the sample. These long times are, however, typical for relaxation effects of nuclear spin systems. In order to explore the possibility of any such connection, Kronmüller *et al.* [104] performed NMR experiments where the sample is brought to the HLRM state and then an AC magnetic field perpendicular to the static field was created by application of a radio

frequency (rf). In this experiment, it was established that the resistance value of the HLRM drops when rf frequencies correspond to splitting of nuclear spins. These authors therefore concluded that the electron transport in the HLRM state must be related to nuclear spin polarization which might happen when the electrons pass between domains of unpolarized and polarized ground states.

3.5. *The half-polarized states*

As mentioned above, electron spin polarization at various QHE filling factors can be explored experimentally by analysing the circular polarization of time-resolved radiative recombination of two-dimensional electrons with photo-excited holes bound to acceptors. Details on this type of experimental probe can be found in [87, 105, 106]. From the measured luminescence spectra, information about the magnetic field dependence of the electron spin polarization at various quantum Hall states were derived by these authors. Their typical results are shown in figure 32. For

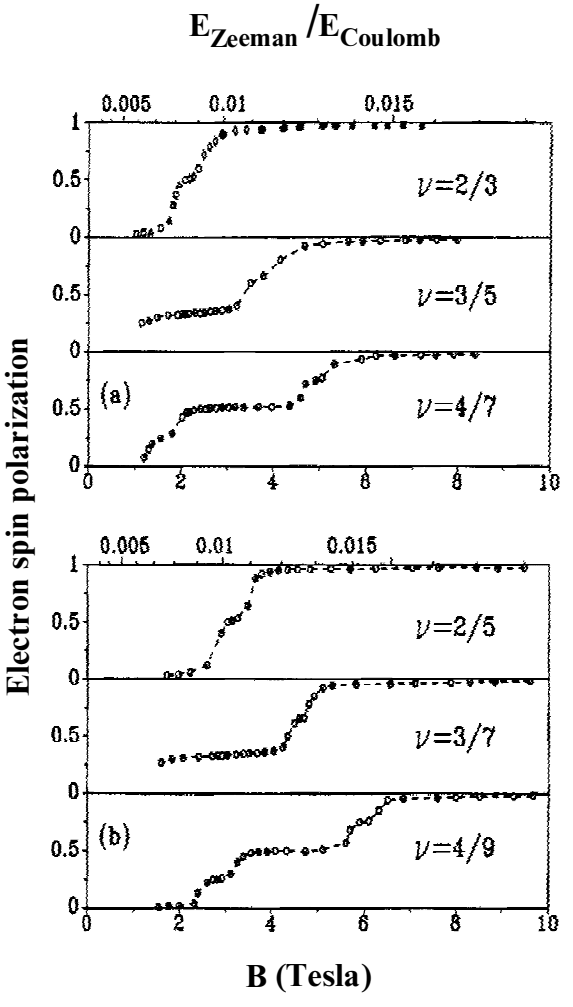

Figure 32. Electron spin polarization as a function of the external magnetic field of various filling factors which show quantum Hall effects [106].

the filling factors $\nu = \frac{2}{3}$ and $\nu = \frac{2}{5}$, the experimental results clearly indicate the expected spin transition from an unpolarized state at low fields to a fully polarized state when the magnetic field is increased. Interestingly, there is also a weak structure visible midway between the two prominent phases. This weak structure corresponds to half the maximal spin polarization.

Observation of these half-polarized states is quite remarkable because their presence at these two filling factors cannot be explained by any conventional theoretical approaches which are currently available [107]. For higher order filling factors, many more intermediate spin polarizations are also clearly visible (figure 32).

3.6. *Spin properties of a system at* $\nu = 1$

Lately, it has been realized that the innocuous lowest odd integer filling factor, which was thought to have the simplest and a rather benign state, has interesting spin-related effects in the ground state as well as in the low-lying excitations. In our discussions of the $\nu = 1$ state that follow, we consider the case of zero Zeeman splitting. In the presence of interparticle interactions, which we consider to be Coulombic, the system can in fact, lower its interaction energy by maximizing its total spin (Hund's rule). This is because states with maximum total spin are symmetric under spin exchange and hence the spatial part of the wave function is fully antisymmetric. In the lowest Landau level, the kinetic energy is a constant and the system is fully spin polarized.

The spatial part of the wave function is a Vandermonde determinant [19]

$$\Psi \equiv \prod_{i<j} (z_i - z_j) \prod_k \exp(-|z_k|^2/4\ell_0^2),$$

which is the Laughlin wave function for a filled Landau level [16]. In this case, the total spin is $S = n_e/2$ and $S_z\Psi = (n_e/2)\Psi$. The corresponding pair-correlation function is [16, 10]

$$g(|\mathbf{r} - \mathbf{r}'|) = 1 - \exp(-|\mathbf{r} - \mathbf{r}'|^2/2\ell_0^2).$$

The exchange energy is then calculated from

$$E_{ex} = \frac{e^2}{\epsilon\ell_0}\left(\frac{\pi}{2}\right)^{1/2} \sim 64\ \mathrm{K}[B(\mathrm{tesla})]^{1/2},$$

where the energy is in Kelvin and we have considered the parameter values for GaAs. This is also the energy of the lowest-lying charged excitation with a single flipped spin (in the absence of Landau level mixing) [38]. Inclusion of the contribution from the Landau level mixing causes a rapid decrease of the spin-reversed excitation energy, as demonstrated in the Monte Carlo results of [66] and reproduced in figure 33.

The above discussion for $\nu = 1$ cannot be extended to general filling factors. It should be kept in mind that Hund's rule, which suggests that the ground state should have the maximum total spin quantum number consistent with the Pauli principle, does not always apply to two-dimensional electron systems in a strong magnetic field. In fact, we have already noticed that at certain filling factors incompressible ground states do occur which are singlets. These states appear because of electron correlations which dictates that staying in the lowest Landau level is less beneficial for the spin-unpolarized states than for the spin polarized states.

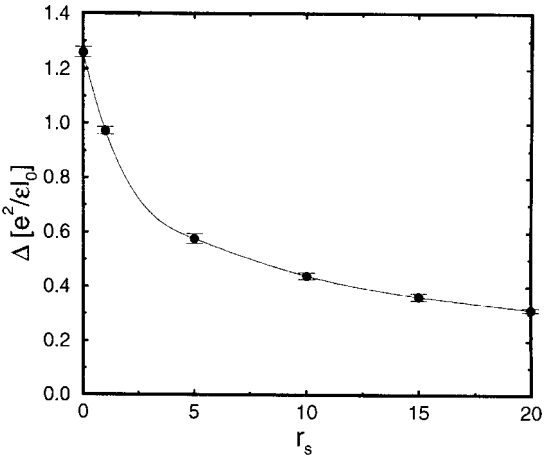

Figure 33. Monte Carlo results for the energy to create a well-separated (spin reversed) quasielectron–quasihole pair at $\nu = 1$ as a function of r_s [66].

The temperature dependence of the spin polarization at $\nu = 1$ was calculated theoretically by the exact diagonalization method applied to finite-size systems in a periodic rectangular geometry [108], as described above for the fractional filling factors. The results for $\langle S_z \rangle$ versus T (in units of $e^2/\epsilon\ell_0$) is shown in figure 34 (*a*) for an eight-electron system at $\nu = 1$. Here the value of the magnetic field is kept fixed

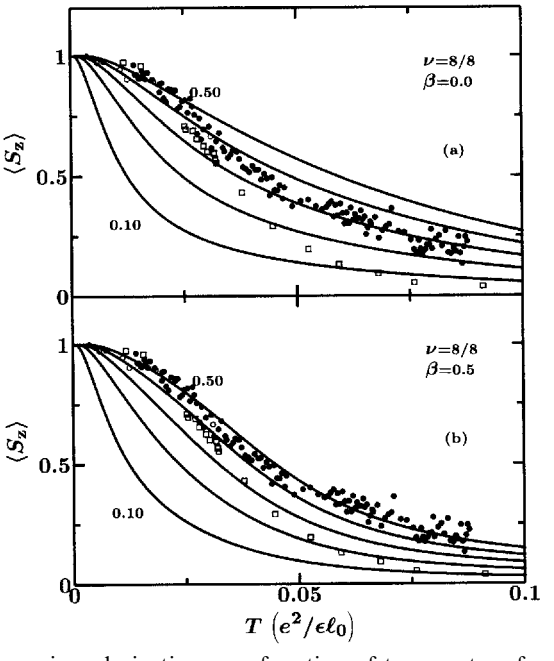

Figure 34. Electron spin polarization as a function of temperature for a six-electron system at $\nu = 1$ for various values of the g factor, (*a*) without and (*b*) with finite-thickness correction included. Experimental results of (▵) [91] and (○,●) [95,96] are also presented here for comparison [108].

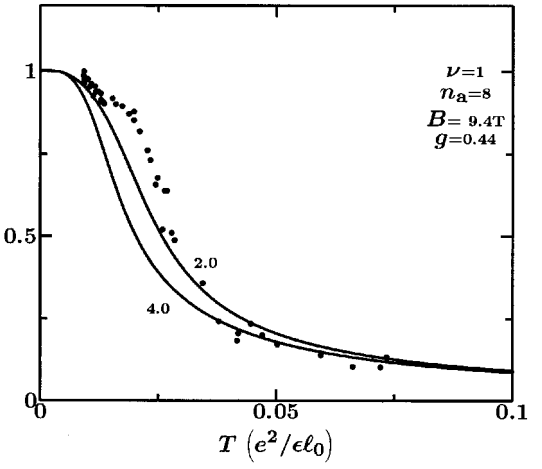

Figure 35. Temperature dependence of the spin polarization at $\nu = 1$ for two different values of the finite-thickness parameter β [113]. Experimental data points are from [112].

(10 T) but we considered different values of the g factor. The experimental results of Barrett *et al.* [91] and the results from magnetoabsorption spectroscopy [95, 96] are also included here for a comparison. Clearly, the observed data show a much sharper drop with increasing temperature than our theoretical results. However, when we include the finite-thickness corrections (figure 34(*b*)), agreement with the experimental results improves significantly. In addition to this theoretical work, there are also calculations for the temperature dependence of the spin polarization at $\nu = 1$, which involve a continuum quantum field theory of a ferromagnet as a model and its properties at finite temperatures [109]. The other work was based on a many-body perturbation theory [110, 111]. The agreement between the calculated temperature dependence of the spin polarization from these theories and the observed results are not very satisfactory.

In a recent paper, Song *et al.* [112] reported NMR spectroscopy in a somewhat similar set up as that of Barrett *et al.* [91] in order to explore $\nu = 1$ (figure 35) and $\nu = 3$ (figure 36). Interestingly, the temperature dependence of the spin polarization at $\nu = 3$ revealed a different behaviour as compared to that at $\nu = 1$. More specifically, the results of Song *et al.* indicated that even at the lowest temperature studied, electron spin polarization at $\nu = 3$ does not show any indication of saturation and with increasing temperature it sharply drops down to zero.

Motivated by these interesting experimental results of Song *et al.*, Chakraborty and Pietiläinen [113] studied the temperature dependence of the spin polarization at higher Landau levels. As discussed above, in this type of work energies are evaluated via exact diagonalization of a few electron system in a periodic rectangular geometry [16]. Since even at the lowest experimental magnetic field the Landau level separation $\hbar\omega_c$ is still an order of magnitude greater than typical energies due to the Coulomb interaction, electrons in the lowest Landau level can be treated as inert. In the calculations that follow we can therefore consider the lowest Landau level to be an uniform background causing merely a constant shift to the interaction energies. The higher Landau levels then enter the system Hamiltonian via a modified interaction potential [114]. More specifically, for a finite number of active electrons n_a in a rectangular cell (correspondingly, $2n_a/(\nu - 2)$ number of inert electrons in the filled

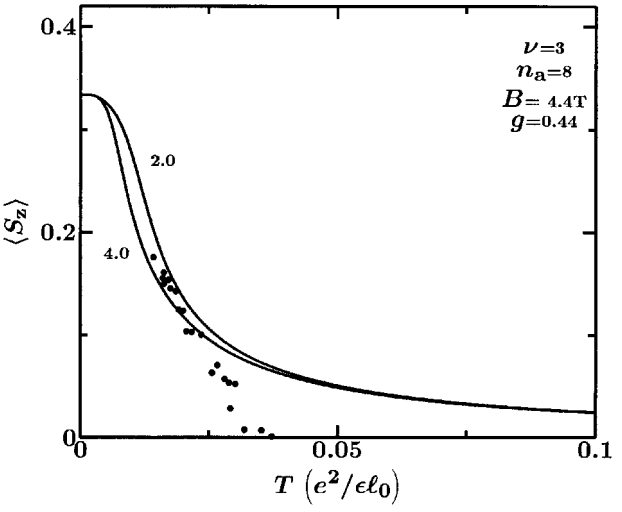

Figure 36. Temperature dependence of the spin polarization at $\nu = 3$ for different values of β [113]. Experimental results are from [112].

level) and choosing the Landau-gauge vector potential, the Hamiltonian in the $n_L = 0, 1$ Landau levels is (ignoring the kinetic energy and single-particle terms in the potential energy which are constants [16]—see equation (6)),

$$\mathcal{H} = \sum_{j_1, j_2, j_3, j_4} \mathcal{A}_{nj_1 nj_2 nj_3 nj_4} a^\dagger_{nj_1} a^\dagger_{nj_2} a_{nj_3} a_{nj_4},$$

$$\mathcal{A}_{nj_1 nj_2 nj_3 nj_4} = \delta'_{j_1+j_2, j_3+j_4} \mathcal{F}_n(j_1 - j_4, j_2 - j_3),$$

$$\mathcal{F}_n(j_a, j_b) = \frac{1}{2ab} {\sum_{\mathbf{q}}}' \sum_{k_1} \sum_{k_2} \delta_{q_x, 2\pi k_1/a} \delta_{q_y, 2\pi k_2/b} \delta'_{j_a k_2}$$

$$\times \frac{2\pi e^2}{\epsilon q} \left[\frac{8 + 9(q/d) + 3(q/d)^2}{8(1 + q/d)^3} \right]$$

$$\times \mathcal{B}_n(q) \exp(\tfrac{1}{2} q^2 \ell_0^2 - 2\pi i k_1 j_b / n_s),$$

$$\mathcal{B}_n(q) = \begin{cases} 1, & \text{for } n_L = 0, \\ (1 - \tfrac{1}{2} q^2 \ell_0^2)^2, & \text{for } n_L = 1, \end{cases}$$

$$n_e = \begin{cases} n_a, & \text{for } n_L = 0, \\ \dfrac{\nu}{\nu - 2} n_a, & \text{for } n_L = 1. \end{cases}$$

Here, as earlier, a and b are the two sides of the rectangular cell which contains the electrons. The Fang–Howard variational parameter d is associated with the finite-thickness correction [16], ϵ is the background dielectric constant, and the results are

presented in terms of the dimensionless thickness parameter $\beta = (d\ell_0)^{-1}$. The Kronecker δ with prime means that the equation is defined mod n_s, and the summation over q excludes $q_x = q_y = 0$. As discussed in section 2.2, this numerical method has been widely used in the quantum Hall effect literature [16] and is known to be very accurate in determining the ground state and low-lying excitations in the system.

Results for $\langle S_z(T)\rangle/\max\langle S_z(T)\rangle$ versus T for an eight-electron system in a periodic rectangular geometry at $\nu = 1$ are presented in figure 35 where we also present the experimental data of [112] for comparison. Here the temperature is expressed in units of $e^2/\epsilon\ell_0$ and the conversion factor to Kelvin is $e^2/\epsilon\ell_0[\mathrm{K}] = 51.67(B[\mathrm{tesla}])^{1/2}$, which is appropriate for the system studied in the experiments. In our calculations, we fix the parameters as in the experimental systems: the Landé g factor is 0.44 and the magnetic field is $B = 9.4\,\mathrm{T}$. The curves that are close to the experimental data (and presented here) are for $\beta = 2$–4. As we discussed above, at low temperatures there is a rapid drop in spin polarization and for high temperatures spin polarizations decay as $1/T$. Our results are in good agreement with these experimental features. They were also in good qualitative agreement with the earlier experimental results at this filling factor [108]. These results are presented with the intention of comparing them with the temperature dependence of the spin polarization at $\nu = 3$. The results in the latter case are shown in figure 36 (again for an eight-electron system in a periodic rectangular geometry). In drawing this figure, we have taken the following facts from the experimental results of [112] into consideration [113]:

(1) that the maximum $\langle S_z\rangle$ is in fact 1/3 and not 1 as in $\nu = 1$,
(2) the experimental scale at $\nu = 3$ of [112] is the same as that at $\nu = 1$, and
(3) spin polarization at $\nu = 3$ is drawn in figure 36 on the same scale as for $\nu = 1$.

All the parameters except the magnetic field are kept the same as in the case of $\nu = 1$. Just as in the experimental situation, we fix the magnetic field for $\nu = 3$ at a much lower magnetic field of $B = 4.4\,\mathrm{T}$. The filled Landau levels, however, are still found to be inert at this low field and this does not influence our chosen Hamiltonian. As seen in figure 35, numerical values of spin polarization are much smaller here than those for $\nu = 1$. Our theoretical results for $\beta = 2$–4 agree reasonably well with the experimental results of [112] except in the high temperature regime where the experimental data drop down to zero. Theoretical results, in contrast, have the usual $1/T$ tail. We should point out however, that owing to discreteness of the energy spectrum for a finite number of electrons the terms with S_z and $-S_z$ in the polarization cancel each other at high temperatures like $1/T$ and we will always end up with $1/T$ decay of $\langle S_z(T)\rangle$ versus T [97]. Therefore, we cannot predict with certainty how a macroscopic system would behave at high T. However, given the fluctuations in data points for $\nu = 1$ and $\nu = 3$ and the fact that the last few data points for $\nu = 3$ are extremely small, it is not clear if one expects saturation of points with $1/T$ behaviour or the spin polarization actually vanishes. Clearly, experimental data at high temperatures do not show any sign of saturation and in order to settle the question of the actual vanishing of $\langle S_z(T)\rangle$ it would be helpful to have more data in the high temperature regime. Saturation is also not visible in the low-temperature region of the experimental data. In order to clarify many of these outstanding issues, it is rather important to have more experimental studies of the temperature dependence at this filling factor.

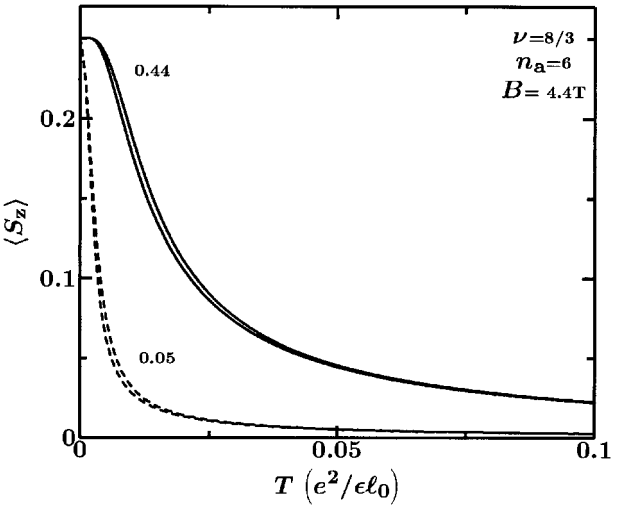

Figure 37. Temperature dependence of the spin polarization at $\nu = \frac{2}{3}$ for $\beta = 2,4$ and two different values of the Landé g factor ($g = 0.44$ and $g = 0.05$). The results are almost independent of β [113].

The influence of higher Landau levels is found to be quite significant for the filling factor $\nu = \frac{2}{3}$ [113]. The results for $\langle S_z(T)\rangle$ versus T at $\nu = \frac{8}{3}$ are shown in figure 37, where we present results for a six-electron system and a magnetic field value of 4.4 T. In figure 37, we present our results for $\beta = 2,4$, but the spin polarization is rather insensitive to the finite-thickness correction. We also consider two different values of Landé g factor: 0.44 (solid curves) and 0.05 (dashed curves). Interestingly, the results indicate that the total spin S of the active electrons, unlike in the lowest Landau level, is at its maximum value $S = n_a/2$ even without Zeeman coupling. Hence even an infinitesimal Zeeman coupling will orient the spins in the active system resulting in the polarization being 1/4. This is at odds with the conventional composite fermion model which predicts fractions of the form $2 + 2/m$, m odd, to be unpolarized [22]. This somewhat surprising behaviour can be thought to be the result of more repulsive effective interactions forcing the electrons, according to Hund's rule, to occupy the maximum spin state more effectively as compared with electrons on the lowest Landau level. In order to demonstrate this behaviour we have considered the case of a very small Zeeman energy (dashed curves), but the results still indicate full spin polarization of the active system. At this low Zeeman energy, spin polarization drops rather rapidly from its maximum value as the temperature is increased.

More experimental data points at $\nu = 3$ in the low- and high-temperature regime would be very helpful. Experimental studies of $\nu = \frac{8}{3}$ with NMR and optical spectroscopy should be able to explore the spin states predicted in [113].

3.7. *Spin excitations near a filled Landau level*

It has long been known that for the odd integer QHE, the energy gaps measured in transport experiments [115] exceed the single-particle Zeeman gaps, obtained from *bare* g factors [116] by as much as a factor of 20. This result clearly indicated the important influence of the electron–electron interaction on the energy gaps. In the following discussion of spin excitations around $\nu = 1$ we will try to demonstrate

the significance of that inter-electron interaction. The simplest neutral excitations of the fully spin-polarized ground state at $\nu = 1$ are those with a single reversed spin. They carry charge $\pm e$ and spin $S_z = \frac{1}{2}$ and they have the size of a magnetic length ℓ_0. Interestingly, collective spin-wave dispersion can be calculated analytically [19, 117]

$$E(k) = g\mu_B B + \frac{e^2}{\epsilon \ell_0}\left(\frac{\pi}{2}\right)^{1/2}[1 - \exp(-k^2\ell_0^2/4)I_0(k^2\ell_0^2/4)], \tag{17}$$

where I_0 is the modified Bessel function of the first kind. The neutral excitation at $k = 0$, i.e. the bare gap, $E(0) = g\mu_B B$ can be measured in, e.g. electron spin resonance experiments [116]. On the other hand, transport measurements are sensitive to charged excitations for $k \to \infty$,

$$E(k) \overset{k\to\infty}{=} g\mu_B B + \frac{e^2}{\epsilon \ell_0}\left(\frac{\pi}{2}\right)^{1/2}, \tag{18}$$

where the last term on the right-hand side corresponds to the energy required to separate the quasi electron–hole pair [38]. This spin-wave dispersion seems to account (with the finite-thickness correction included) for the many-body enhancement of the spin gap at $\nu = 1$, which is deduced from the thermally activated transport measurements.

It has been proposed theoretically [118, 119] that in the limit of vanishingly small Zeeman energy, while the ground state at $\nu = 1$ is always ferromagnetic, the lowest energy charged excitations are different from a quasi electron–hole pair. These quasiparticles cover an extended region and have a non-trivial spin order; these are the so-called skyrmions. In this case, excitations still carry charge $\pm e$ but at the boundary of the system the local spin takes the value of the ground state and is reversed at the centre of the skyrmion. Along any radius, the spin gradually twists between these two limits. Although flipping many spins in the skyrmionic picture costs more Zeeman energy, the fact that neighbouring spins are nearly parallel saves on exchange energy. The size of the skyrmion is determined by the competition between the interaction energy and the Zeeman energy. The former favours a large size in order to have uniform charge density, while the latter, with increasing field strength, tends to reduce the size.

The energy to create a skyrmion–antiskyrmion pair has been calculated by Sondhi *et al.* [118]

$$E(g) = \frac{1}{2}\left(\frac{\pi}{2}\right)^{1/2}\frac{e^2}{\epsilon \ell_0}\left[1 + \frac{3\pi}{4}\left(\frac{18}{\pi}\right)^{1/6}\left(\frac{\epsilon a}{\ell_0}\right)^{1/3}(g|\ln g|)^{1/3}\right], \tag{19}$$

where $a = \hbar^2/me^2$ is the Bohr radius. At $g = 0$, equation (19) predicts a gap that is half the energy to create a pair of single-particle excitations.

On the other hand, it has been noted by some authors that Landau level mixing (LLM) has a significant effect on the spin gap at $\nu = 1$. Using a variational quantum Monte Carlo approach Kralik *et al.* [120, 121] calculated the influence of Landau level mixing on the single spin-flip gap. In their approach, LLM was incorporated by multiplying the lowest Landau level wave function with a Jastrow factor

$$\Psi = \psi_J \psi_{\mathrm{LLL}}, \quad \psi_J = \prod_{i<j} \exp[-u(|\mathbf{r}_i - \mathbf{r}_j|)]$$

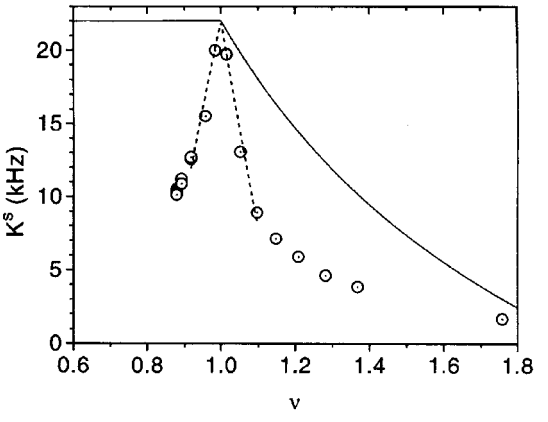

Figure 38. Filling factor dependence of K_s for $B = 7.05\,\mathrm{T}$ at 1.55 K. The solid line depicts what one expects for the non-interacting electron system and the dashed-line is for finite-size skyrmions [91].

and a parametrized function was adopted for the pseudopotential $u(r)$. The spin gap was defined as the discontinuity in the chemical potential across the $\nu = 1$ state. These authors found that the effect of the Jastrow factor was to decrease the spin gap quite significantly at low magnetic fields. For low r_s†, the spin-flip energy with Landau level mixing included is much lower than the $k \to \infty$ energy of the spin wave dispersion (equation (18)), and also much lower than the Hartree–Fock energy of a skyrmion–antiskyrmion pair appropriate for finite g [119], and lower than the energy calculated by Sondhi *et al.* A very significant conclusion, which was derived from the work of Kralik *et al.*, was that energetically, single spin flip excitations might be a better candidate compared to skyrmions for lowest energy excitations at $\nu = 1$ under appropriate conditions.

Experimental evidence for excitations near $\nu = 1$ which involve multiple spins came from the pioneering work of Barrett *et al.* [91] described in section 3.1. Their results for Knight shift $K_s(\nu)$ for $B = 7.05\,\mathrm{T}$ at $T = 1.55\,\mathrm{K}$ are shown in figure 38. These results clearly do not agree with the non-interacting electron picture (solid curve). Instead, when one moves slightly away from $\nu = 1$, rapid depolarization indicates charge excitations of the $\nu = 1$ ground state, which have an effective spin of $(3.6 \pm 0.3)/2$. Supporting evidence of such multi-spin excitations came from subsequent magnetoluminescence studies [95, 96, 122] and transport measurements [123, 124].

A large reduction of the spin polarization observed near $\nu = 1$ should also be expected near $\nu = 3$ because in this case the two lower Landau levels are fully filled and would be inert as mentioned above. Theoretical works [125, 126] however predicted that skyrmion excitations are energetically unfavourable for $\nu = 3$, 5 and 7, even in the limit of vanishing Zeeman energy. Cooper [127] extended these calculations by including finite-thickness corrections and concluded that these corrections should be able to make skyrmion excitations favourable for odd integer filling factors. In the NMR experiments of Song *et al.* [112] discussed above, the ^{71}Ga NMR results did show a significant reduction of electron spin polarization when one

† r_s is defined in section 2.3.1.

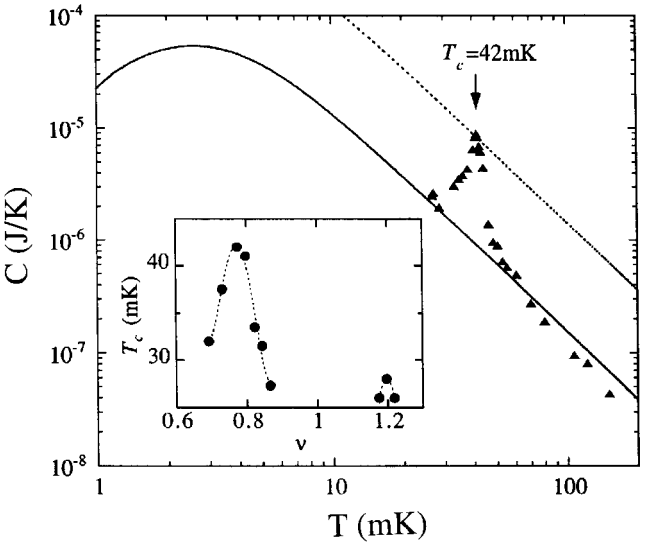

Figure 39. Measured heat capacity C versus temperature at $B = 8.5\,\mathrm{T}$ and $\theta = 30^\circ$ ($\nu = 0.77$). The solid line is the calculated Schottky nuclear heat capacity of the GaAs 100 QWs and the dotted line corresponds to that for a 100-period GaAs heterostructure. Measured ν dependence of T_c at $\theta = 30^\circ$ is shown as an inset [128,129].

moved away from $\nu = 3$. These results were interpreted as evidence for the existence of skyrmion excitations near $\nu = 3$.

Analysis of circular polarization of time-resolved luminescence by Kukushkin *et al.* [87, 88] (see section 2.7) however revealed a very different picture. In these experiments, spin excitations around $\nu = 1$ were investigated for very low magnetic fields (ratio of Zeeman to Coulomb energies were ~0.005–0.009). The results clearly indicated only single spin-flip excitation rather than rapid depolarizations around $\nu = 1$. It is possible that the Landau level mixing becomes very important at these low fields and single spin-flip excitations are energetically preferred, as suggested by the work of Kralik *et al.* [120, 121].

It is well known that the measurement of heat capacity of a 2DES can provide important information about the Landau quantized density of states and the quantum Hall effects. The heat capacity results (figure 39) on a multiple-quantum-well sample in the quantum Hall regime exhibit several unusual features [128, 129]. At high temperatures ($\simeq 70\,\mathrm{mK}$) the measured data are consistent with the calculated Schottky nuclear heat capacity of Ga and As atoms in the quantum wells (QWs) [128]. At lower temperatures, however, C exceeds the calculated value by a factor of up to ~10 at T_c. It should be noted that the *peak* value of the heat capacity appears consistent with the Schottky nuclear heat capacity of the heterostructure if the nuclei of the barrier atoms are also included (dotted line). This suggests that the peak might arise from the contribution of nuclear spins of the barrier nuclei.

The NMR experiments in [93] indicated that nuclear spin diffusion from the quantum wells into the barrier is very weak, except when optical pumping broadens the Knight shift peak which then overlaps with the NMR peak of the barrier. This type of spectral overlap can allow spin diffusion which is driven by the nuclear magnetic dipole coupling. Enhancement of spin diffusion across the QW–barrier

interface near T_c could therefore originate from a broadening of the Knight shift peak in the QWs as discussed above. In a liquid skryme phase, motional averaging of the 2DES spin polarization would produce a single Knight shift [91]. In the case when the skrymions are in a lattice state there is no motional averaging and depending upon the local spin polarization of the 2DES, one can have both positive and negative Knight shifts. As the experimental results indicate that above and below the peak in C versus T the spin diffusion across the QW–barrier interface is very weak, there is no overlap of the Knight shift peak and the NMR peak of the barrier in *both* the liquid and solid skryme phase. It has been speculated [130] that the peak is associated with the liquid–solid phase transition of the skyrmion system.

Melinte *et al.* [131] reported recent results on low-temperature heat capacity measurements on a GaAs–AlGaAs multiple quantum-well heterostructure with Zeeman energy tuned by tilting the sample in the magnetic field. They noticed that the nuclear contribution to heat capcaity decreases in the range $0.037 \leq \tilde{g} \lesssim 0.043$, where $\tilde{g} = |g^*|\mu_B B/(e^2/\epsilon\ell_0)$, and suppressed for $\tilde{g} \gtrsim 0.04$. This observation was interpreted as evidence for a transition from skyrmions to single spin-flip excitations at $\tilde{g}_c \approx 0.04$. This critical $\tilde{g}$ is somewhat smaller than the theoretical estimates [127].

Finally, Dolgopolov *et al.* [132] reported a direct measurement of the spin gap via magnetocapacitance techniques. The gap was derived from the gate voltage dependence of the electron density in the two-dimensional electron gas of the sample. In the magnetic field range $5 \leq B \leq 15\,\mathrm{T}$, the spin gap displayed a linear dependence on the magnetic field, just like in activation energy measurements, and corresponds to an enhanced Landé factor $g \approx 5.2$. Neither the skyrmion model, nor the model of the exchange-enhanced g factor can explain the observed results. To sum up this section: it is fair to conclude that despite a profusion of experimental and theoretical activities, mystery of the spin gap at $\nu = 1$ still remains largely unresolved.

3.8. *Spin transitions in a $\nu = 2$ bilayer* QH *system*

Inelastic light scattering by a 2DEG is capable of probing excitations in the system over a wide range of wave vectors [133]. It can measure the spin-density and charge-density collective modes, as well as single-particle excitations. It has long been known [134] that in a double-layer QHE system, interlayer electron correlations are responsible for interesting physical effects such as the appearence of new incompressible states. Experimentally it is now possible to create structures where the two electron layers are separated by a distance which is comparable to intralayer electron separation [34, 135]. Amazingly, in these experiments the individual layers can be controlled independently. In a double-layer system, interlayer spin-dependent correlations can be comparable to intralayer correlations (even in the case of weak interlayer tunnelling). When each layer has one spin-split Landau level occupied ($\nu = 2$), resonant inelastic light scattering studies [136] indicated that the spin density excitations soften to as low as *one-tenth* of the zero-magnetic field results. The extremely low energy was, in fact, close to the Zeeman energy, calculated with $g = -0.4$. The collapse of the spin-density mode with $\delta S_z = 0$ to an energy close to the Zeeman splitting has been attributed to instabilities associated with the emergence of $\delta S_z = 1$ spin-flip excitations.

Sawada *et al.* performed transport measurements on a bilayer QH system [137]. They measured the width of the Hall plateau and activation energy at $\nu = \frac{2}{3}$, 1 and 2 by changing the total electron density and the density ratio in the two quantum wells.

The experimental conditions were such that both the Zeeman energy and the tunnelling energy were much smaller than the Coulomb energy. The $\nu = \frac{2}{3}$ state was found to be a compound state $\nu = \frac{1}{3} + \frac{1}{3}$ which was stabilized entirely by the interlayer Coulomb interaction. Interestingly, the $\nu = 2$ quantum Hall state undergoes a phase transition from a compound state $\nu = 1 + 1$ (spin polarized) to a spin unpolarized state, as the interlayer Coulomb interaction was increased over the intralayer interaction by decreasing the total density. The $\nu = 1$ QH state was, as expected [134, 135], stabilized entirely by the interlayer Coulomb interaction.

3.9. *Spin effects in a narrow* QH *channel*

Theoretical studies of a system of electrons interacting via the long-range Coulomb potential in a narrow channel and in the quantum Hall regime have uncovered a lot of interesting physics [138,139]. These studies indicated that as the interaction strength was increased, abrupt jumps occurred in the expectation values of translationally invariant states. The width of the charge–density profile also displayed similar abrupt changes [138]. The phase diagram of stable 1D-FQHE states were calculated and interestingly, the lowest half-filled Landau level appeared as a stable incompressible state under certain conditions. Experimental observation of a signature of the FQHE in a narrow channel was, in fact, reported a few years before [140].

Recent theoretical work on the QHE in a narrow channel [138, 139] revealed that the temperature dependence of the electron spin polarization for a narrow quantum Hall system shows behaviour analogous to that of a two-dimensional system at major filling factors. At the lowest half-filled quantum Hall state for which no two-dimensional analogue exists, we find a stable spin partially-polarized system [138].

In our model for the QHE in a narrow channel, we consider a finite number of spin polarized electrons interacting via the long-range Coulomb potential [138] and confined by a potential which is parabolic [141] in one direction and flat in the other. A strong magnetic field is applied perpendicular to the xy plane. The electrons are confined in a cell of length a in the x direction and the width of the cell depends on the strength of the confining potential $(\frac{1}{2}m^*\omega_0^2 y^2)$ relative to the strength of the interactions and also on the length of the cell. We impose a periodicity condition in the x direction. For example, we use antiperiodic boundary conditions for $4n_e$ electrons so that the non-interacting ground states have zero total momentum [138].

Electrons are assumed to occupy only the lowest Landau level owing to the strong magnetic field. The effective magnetic length in the problem is $\lambda = (\hbar/m^*\Omega)^{1/2}$, where m^* is the electron effective mass, $\Omega = (\omega_0^2 + \omega_c^2)^{1/2}$ and $\omega_c = eB/m^*$ is the cyclotron frequency. The single-electron wave functions are plane waves in the x direction and oscillator wave functions in the y direction centred at $y_0 = 2\pi\lambda^2 m/(a[1 + (\omega_0/\omega_c)^2]^{1/2})$. Here m is the momentum quantum number. The corresponding energies, excluding the constant Landau level energy, are: $E = (2\pi)^2(\lambda/a)^2 m$ in units of $E_0 = (\hbar^2/2m^*\lambda^2)(\omega_0^2/\Omega^2)$. The Hamiltonian in the lowest Landau level, which includes contributions from the electron–electron interactions and the neutralizing background, is numerically diagonalized for a few-electron system with the spin degree of freedom properly included. A phase diagram is then obtained by plotting the energy gap (energy separation between the translationally invariant ground state and the lowest excited state) [138] for various values of a and the increasing strength of the interaction $\mathcal{E}_c = e^2/\epsilon\lambda$ with respect to the energy unit E_0. We should point out that the evaluation of filling factors in a 1D

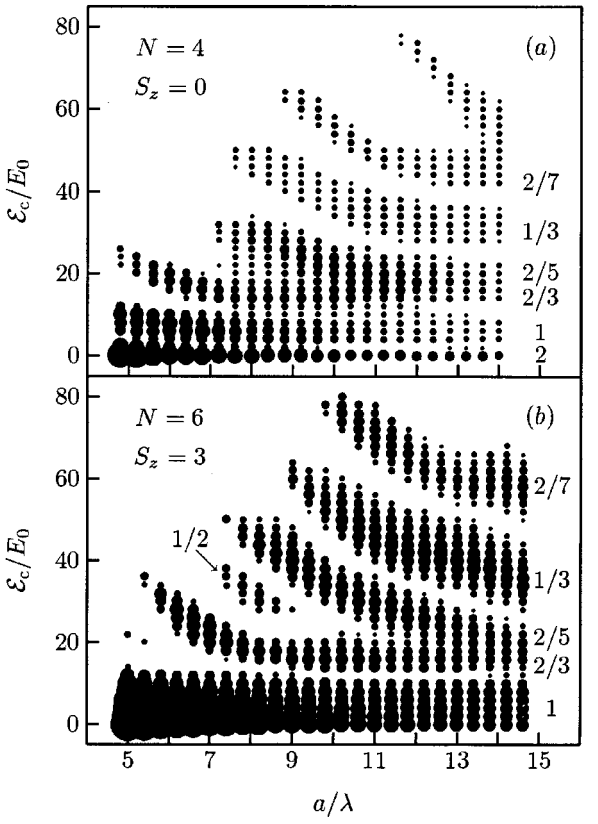

Figure 40. Phase diagram for electrons in an impurity-free narrow channel quantum Hall system (*a*) with and (*b*) without spin degree of freedom included.

system is somewhat tricky. Here the single-particle states corresponding to a particular Landau 'level' are not degenerate. One way is to calculate the areal electron density and number of fluxes through a unit area and determine ν as the ratio of these two quantities. Alternatively, we count the number of occupied states and divide the number of electrons by that. Both methods are somewhat arbitrary: one has to choose properly either the width of the density profile in the first case (we have used full width at half maximum) or, in the second approach, which state should be considered as occupied. We have checked that both methods agree reasonably well. The $\frac{1}{3}$ FQH state in the present system is also identified from the momentum distribution function $\langle n(k)\rangle = \langle 0|a_k^\dagger a_k|0\rangle$ by comparing it with that for a Laughlin-like wave function.

In figure 40, we present the results for the phase diagram, calculated for (a) a system of four electrons with $S_z = 0$ (Zeeman energy not included) and (b) a system of six spinless electrons, for $\alpha = \omega_0/\omega_c = 0.23$ which is appropriate for $B = 10$ T and $\hbar\omega_0 = 4$ meV. The area of a filled dot is directly proportional to the energy gap. As is evident in the figure, several quantum Hall states are stable with large energy gaps in the parameter range considered in this work. For the $N = 4$ system the $\nu = \frac{1}{2}$ state, which exists for the spinless system, cannot be resolved in this phase diagram. In figure 40 (*a*), the $\nu = \frac{1}{2}$ states are expected to lie between $\nu = \frac{2}{3}$ and $\nu = \frac{2}{5}$. In general,

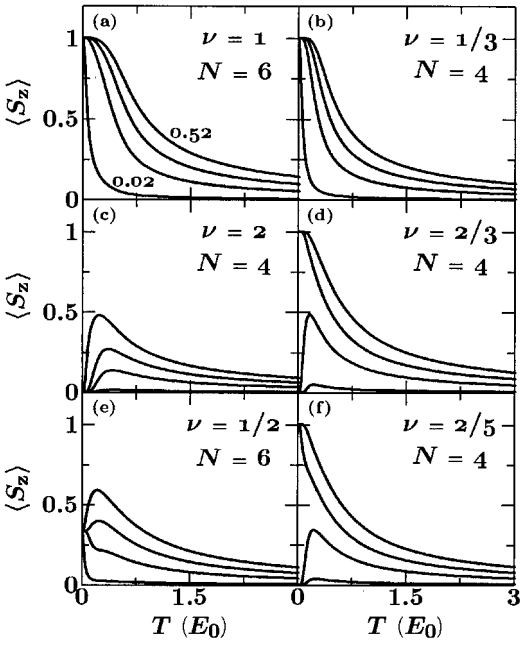

Figure 41. Spin polarization $\langle S_z \rangle$ versus T for $\nu = 1$, 2, $\frac{2}{3}$, $\frac{2}{3}$, $\frac{1}{2}$, $\frac{1}{3}$ and $\frac{2}{5}$ for a narrow channel QHE system at various values of the g factor.

the energy gaps are larger for spinless electrons (figure 40 (*b*)) because in the other case there are low-lying spin excitations available.

Results for $\langle S_z(T) \rangle$ versus T at $\nu = 1$, 2, $\frac{2}{3}$, $\frac{2}{5}$, $\frac{1}{3}$ and $\frac{1}{2}$ are shown in figure 41. In these calculations the magnetic field was kept fixed at 10 T and the g factor was varied $(0.02 - 0.52)$. At $\nu = 1$, we find the results to be similar to those for the two-dimensional systems [108] and the system is fully spin polarized even for very low values of the Zeeman energy. Qualitatively similar behaviour is also seen at $\nu = \frac{1}{3}$. In the same way, $\nu = 2$ is a spin-unpolarized state even at the highest value of the Zeeman energy considered and $\nu = \frac{2}{3}$ and $\nu = \frac{2}{5}$ are spin-unpolarized states at low Zeeman energies with a non-monotonic temperature dependence as predicted for a 2DES [97] (see section 3.2). As discussed above, such a non-monotonical behaviour has been observed in experiments on a 2DES [87]. The clear correspondence with the spin polarization in a two-dimensional system gives us confidence that our classification of the QH states in a narrow channel system is essentially correct. At $\nu = \frac{1}{2}$ we find a spin partially-polarized state. An experimental probe of the narrow channel QHE states would be very useful for understanding the physics of half-filled states [139], as predicted theoretically.

3.10. *Spin effects near a compressible state*

In recent years, a modified Fermi liquid theory of Chern–Simons fermions, put forward by Halperin *et al.* [28, 142], has proven to be a useful formalism in understanding the nature of even-denominator filling factors such as $\nu = \frac{1}{2}, \frac{3}{2}$, etc. A detailed account of this theory is available in several excellent articles [28, 142,143]. We present below only the essential elements of this work. The approach is essentially a transformation where each electron is converted to a fermion attached

to a δ-function flux of size $2m\Phi_0$, where m is an integer and Φ_0 is the flux quantum. The transformation (sometimes described as a singular gauge transformation) corresponds to a change in phase of the many-electron wave function. As a result, only the kinetic energy term [31] of the electron Hamiltonian is modified. This term includes, in addition to the electromagnetic vector potential resulting from the externally applied magnetic field, an additional vector potential which depends on the position of the particles.

A simple way to deal with the transformed fermion system is to make a *mean-field approximation* where the inter-particle interaction is turned off, the density of the transformed particles is assumed to be uniform and the fictitious flux quanta attached to the fermions are smeared out into an uniform field. Then when the electron filling factor is $\nu = 1/2m$ and the sign of the attached flux is chosen appropriately, the externally applied magnetic field is cancelled, on average, by the fictitious field. The non-interacting fermions may then form a filled Fermi sea—a compressible state. When the electron filling factor differs from $\nu = 1/2m$, the fermions see a net field and since we are dealing with a system of non-interacting fermions in a uniform field, at $\nu = p/(2mp + 1)$, p being an integer, the transformed fermions will fill $|p|$ Landau levels (corresponding to the residual magnetic field), in agreement with the composite fermion picture of Jain [21].

The mean-field approximation described above is rather crude and can only be justified as an initial step toward a complete theory for the interacting system of fermions. In particular, contributions from the terms which are neglected in the many-particle Hamiltonian, namely, the interparticle interaction and the correct flux-field vector potential which depends on the positions of all the particles, need to be estimated. Interestingly, as explained below, the spin-related effects observed in recent experiments have put the mean-field approximation to a severe test.

Du *et al.* [144] and Störmer and Tsui [145] have recently performed the angular-dependent transport measurements of various fractional quantum Hall states. The re-entrant behaviour observed at various fractions around $\nu = \frac{3}{2}$ was interpreted via a simple picture of composite fermions (CF) with a spin. Using the mean-field picture of CFs described above, these authors described spin polarization of the CF system at any FQHE state and Zeeman energy in terms of the crossings of spin-split Landau levels from different CF Landau levels. A problem remains, however, with the spin polarization at $\nu = \frac{3}{2}$. Analysis by these authors indicates a partially polarized state. Experimental results [146] have, however, long asserted that the system is fully spin polarized. In fact, in the electron system $\nu = \frac{3}{2}$ is particle–hole symmetric to $\nu = \frac{1}{2}$, itself a spin polarized system. In the CF picture, $\nu = \frac{3}{2}$ is a filled Fermi sea and the particle–hole symmetry is not applicable. It is to be emphasized that the interparticle interaction is ignored in this scheme. Instead, some suitable *effective* parameters, such as g^* or m^* are introduced to determine the spin polarization. The discrepancy between the CF prediction and experiments at $\nu = \frac{3}{2}$ is most likely the result of an unknown behaviour of these parameters. On the other hand, the discrepancy might also indicate that the simple-minded CF picture needs to be generalized by including the mutual interaction between the composite fermions. However, the nature of this interaction is not known. We wish to point out that a similar situation exists at the half-polarized state described in section 3.5, where the non-interacting CF system fails to explain the experimental results [107, 147, 148].

4. Summary and open questions

Fractional QHE has come a long way since the original discovery in 1982. Although the Nobel prize to Laughlin was a recognition of his monumental contribution in providing a theoretical explanation of the primary $\frac{1}{3}$ state and introduction of fractionally-charged quasiparticles in the system, a satisfactory theoretical understanding of the effect in its present state, which has grown significantly into a vast field, is still a long way off. However, as we have tried to demonstrate in this review, one aspect of this effect, namely, the importance of the spin degree of freedom (and its various implications) is quite well established and is an important consequence of the effect. New and ingenious experiments, which are regularly reported in the literature, have provided a clear picture of this aspect of the FQHE. It is now firmly established from all these experiments that for filling factors $\nu = \frac{2}{3}, \frac{2}{5}, \frac{3}{5}$, etc., the ground state and low-lying excitations involve spin reversal, as predicted theoretically. Similarly, the ground states of $\nu = 1, \frac{1}{3}$, etc., are fully spin polarized, but low-energy excitations are spin-reversed quasiparticles in the limit of vanishing Zeeman energy. The temperature dependence of these spin-reversed excitations are also well understood. There are still, however, a lot of problems that need attention.

One important problem is to have a better understanding of the true nature of spin excitations near $\nu = 1$. The role of skyrmionic excitations vis-à-vis the effect of Landau level mixing need to be clarified. Similarly, a sound theoretical foundation for the hysteretic behaviour observed at $\nu = \frac{2}{3}$ and $\nu = \frac{3}{5}$ is still lacking. Spontaneous separation of a 2DEG at $\nu = \frac{2}{3}$ into spin domains, which is perhaps reflected in the recent experiments discussed above, is a very intriguing possibility that requires a suitable theoretical understanding.

Observation of the QHE at $\nu = \frac{5}{2}$ and its absence at $\nu = \frac{1}{2}$ is another puzzle which remains to be resolved [14, 34]. Tilted-field experiments by Eisenstein *et al.* [149] revealed a linearly decreasing activation gap with a g factor, derived from the slope, of $|g| \approx 0.56$. This would clearly be an indication that unpolarized (or partially polarized) spin states are involved. However, a re-entrant tilted-field behaviour, which is associated with the partially spin polarized odd-denominator states, is absent for $\nu = \frac{5}{2}$. Theoretical works on this filling factor are also inconclusive about the spin state of this filling factor [114, 150, 151]. A detailed account of the $\nu = \frac{5}{2}$ filling factor can be found in [34]. Spin polarizations of the $\nu = \frac{3}{2}$ state needs a better explanation. Similarly, the recently observed half-polarized states require a clear theoretical understanding. We also expect many more surprises from various filled Landau levels and perhaps, even spin transitions at a half-filled Landau level in a narrow channel. It is indeed interesting to note that what started as a mere consequence of a small g factor has now matured into a state of rich physics where intricate roles are played by Zeeman energy, electron correlations, NMR, hydrostatic pressure, and many other factors. The chapter on spin effects in a QH system is far from being closed.

Acknowledgements

I would like to thank the Oulu group: Pekka Pietiläinen, Veikko Halonen, and Karri Niemelä for their valuable input in the review. I thank Silvia Kronmüller (Max Planck Institute, Stuttgart) for helpful discussions on the hysteretic behaviour and Peter Maksym (Leicester) for helpful comments. I also thank Peter Fulde for his

kind hospitality at the Max Planck Institute, Dresden where a large part of the review was written.

References

[1] TSUI, D., STORMER, H. L., and GOSSARD, A. C., 1982, *Phys. Rev. Lett.*, **48,** 1559.
[2] VON KLITZING K., DORDA, G., and PEPPER, M., 1980, *Phys. Rev. Lett.*, **45,** 494.
[3] TSUI, D., and STORMER, H. L., 1986, *IEEE J. quantum Electron.*, **22,** 1711.
[4] STORMER, H. L., 1984, *Festkörperprobleme/Advances in Solid State Physics*, Vol. 24, edited by P. Grosse (Braunschweig: Vieweg), p. 25.
[5] STORMER, H. L., 1992, *Physica* B, **177,** 401.
[6] STORMER, H. L., TSUI, D. C., and GOSSARD, A. C., 1999, *Rev. mod. Phys.*, **71,** S298.
[7] STORMER, H. L., 1999, *Rev. mod. Phys.*, **71,** 875.
[8] LAUGHLIN, R. B., 1999, *Rev. mod. Phys.*, **71,** 863.
[9] TSUI, D., 1999, *Rev. mod. Phys.*, **71,** 891.
[10] LAUGHLIN, R. B., 1983, *Phys. Rev. Lett.*, **50,** 1395.
[11] CLARK, R. G., NICHOLAS, R. J., USHER, A., FOXON, C. T., and HARRIS, J. J., 1986, *Surf. Sci.*, **170,** 141.
[12] WILLETT, R., EISENSTEIN, J. P., STORMER, H. L., TSUI, D. C., GOSSARD, A. C., and ENGLISH, J. H., 1987, *Phys. Rev. Lett.*, **59,** 1776.
[13] CHANG, A. M., BERGLUND, P., TSUI, D. C., STORMER, H. L., and HWANG, J. C. M., 1984, *Phys. Rev. Lett.*, **53,** 997.
[14] SAJOTO, T., SUEN, Y. W., ENGEL, L. W., SANTOS, M. B., and SHAYEGAN, M., 1990, *Phys. Rev.* B, **41,** 8449.
[15] LAUGHLIN, R. B., 1990, *The Quantum Hall Effect*, 2nd edn, edited by R. E. Prange and S. M. Girvin (Berlin: Springer-Verlag).
[16] CHAKRABORTY, T., and PIETILÄINEN, P., 1995, *The Quantum Hall Effects*, 2nd edn (New York: Springer).
[17] CHAKRABORTY, T., 1992, *Handbook on Semiconductors*, Vol. 1, edited by P. T. Landsberg (New York: Elsevier), Ch. 17.
[18] LAUGHLIN, R. B., 1981, *Phys. Rev.* B, **27,** 3383 (1983).
[19] BYCHKOV, YU. A., IORDANSKII, S. V., and ELIASHBERG, G. M., 1981, *JETP Lett.*, **33,** 143.
[20] HALPERIN, B. I., 1983, *Helv. Phys. Acta*, **56,** 75.
[21] JAIN, J. K., 1989, *Phys. Rev. Lett.*, **63,** 199.
[22] DAS SARMA, S., and PINCZUK, A. (eds), 1997, *Perspectives in Quantum Hall Effects* (New York: Wiley).
[23] HANSEN, J. P., and LEVESQUE, D., 1981, *J. Phys.* C, **14,** L603.
[24] BAUS, M., and HANSEN, J. P., 1980, *Phys. Rep.*, **59,** 1.
[25] GOLDMAN, V., 1995, *Surf. Sci.*, **361,** 1; 1997, *Physica* E, **1,** 15; DE-PICCIOTTO, R., REZNIKOV, M., HEIBLUM, M., UMANSKY, V., BUNIN, G., and MAHALU, D., 1997, *Nature*, **389,** 162; 1998, *Physica* E, **3,** 47; SAMINADAYAR, L., GLATTLI, D. C., JIN, Y., and ETIENNE, B., 1997, *Phys. Rev. Lett.*, **79,** 2526.
[26] READ, N., 1994, *Semicond. Sci. Technol.*, **9,** 1859.
[27] CHAKRABORTY, T., 1998, *Phys. Rev.* B, **57,** 8812.
[28] HALPERIN, B. I., LEE, P. A., and READ, N., 1993, *Phys. Rev.* B, **47,** 7312.
[29] READ, N., and REZAYI, E. H., 1994, *Phys. Rev. Lett.*, **72,** 900.
[30] MORF, R., and D'AMBRUMENIL, 1995, *Phys. Rev. Lett.*, **74,** 5116.
[31] CONTI, S., and CHAKRABORTY, T., 1999, *Phys. Rev.* B, **59,** 2867.
[32] CHAKRABORTY, T., and ZHANG, F. C., 1984, *Phys. Rev.* B, **29,** 7032.
[33] MORF, R., and HALPERIN, B. I., 1986, *Phys. Rev.* B, **33,** 2221.
[34] EISENSTEIN, J. P., 1997, *Perspectives in Quantum Hall Effects*, edited by S. Das Sarma and A. Pinczuk (New York: Wiley).
[35] ZHANG, F. C., and CHAKRABORTY, T., 1984, *Phys. Rev.*, B**30,** 7320.
[36] YOSHIOKA, D., HALPERIN, B. I., and LEE, P. A., 1983, *Phys. Rev. Lett.*, **50,** 1219.
[37] BONSALL, L., and MARADUDIN, A., 1977, *Phys. Rev.* B, **15,** 1959.
[38] ZHANG, F. C., and CHAKRABORTY, T., 1986, *Phys. Rev.* B, **34,** 7076.

[39] STÖRMER, H. L., CHANG, A., TSUI, D. C., HWANG, J. C. M., GOSSARD, A. C., and WIEGMANN, W., 1983, *Phys. Rev. Lett.*, **50,** 1953.
[40] DAVIES, A. G., NEWBURY, R., PEPPER, M., FROST, J. E. F., RITCHIE, D. A., and JONES, G. A. C., 1989, *Phys. Rev.* B, **44,** 13128.
[41] RODGERS, P. J., GALLAGHER, B. L., HENINI, M., and HILL, G., 1993, *J. Phys.: condens. Matter*, **5,** L565.
[42] MURAKI, K., and HIRAYAMA, Y., 1998, *Physica* B, **249–251,** 65.
[43] MURAKI, K., and HIRAYAMA, Y., 1998, *Phys. Rev.* B, **59,** R2502.
[44] MURAKI, K., and HIRAYAMA, Y., 1998, *Physica* B, **256–258,** 86.
[45] MAKSYM, P. A., 1989, *J. Phys.: condens. Matter*, **1,** 6299.
[46] XIE, X. C., GUO, Y., and ZHANG, F. C., 1989, *Phys. Rev.* B, **40,** 3487.
[47] BERAN, P., and MORF, R., 1991, *Phys. Rev.* B, **43,** 12 564.
[48] CHAKRABORTY, T., 1990, *Surf. Sci.*, **229,** 16.
[49] ANDO, T., FOWLER, A. B., and STERN, F., 1982, *Rev. mod. Phys.*, **54,** 437.
[50] FANG, F. F., and HOWARD, W. E., 1966, *Phys. Rev. Lett.*, **16,** 797.
[51] ZHANG, F. C., and DAS SARMA, S., 1986, *Phys. Rev.* B, **33,** 2903.
[52] LAUGHLIN, R. B., 1984, *Surf. Sci.*, **142,** 163.
[53] CHAKRABORTY, T., 1985, *Phys. Rev.* B, **31,** 4026.
[54] HALPERIN, B. I., 1984, *Phys. Rev. Lett.*, **52,** 1583, 2390 (E).
[55] GIRVIN, S. M., MACDONALD, A. H., and PLATZMAN, P. M., 1985, *Phys. Rev. Lett.*, **54,** 581.
[56] HALDANE, F. D. M., and REZAYI, E. H., 1985, *Phys. Rev. Lett.*, **54,** 237.
[57] CHAKRABORTY, T., PIETILÄINEN, P., and ZHANG, F. C., 1986, *Phys. Rev. Lett.*, **57,** 130.
[58] CHAKRABORTY, T., and PIETILÄINEN, P., 1986, *Phys. scripta,* **T14,** 58.
[59] BOEBINGER, G. S., CHANG, A. M., STÖRMER, H. L., and TSUI, D. C., 1985, *Phys. Rev. Lett.*, **55,** 1606.
[60] CHAKRABORTY, T., 1984, *Phys. Rev.* B, **34,** 2926.
[61] CHAKRABORTY, T., and PIETILÄINEN, P., 1990, *Phys. Rev.* B, **41,** 10862.
[62] REZAYI, E., 1987, *Phys. Rev.* B, **36,** 5454.
[63] MORF, R., and HALPERIN, B. I., 1987, *Z. Phys.* B, **68,** 391.
[64] YOSHIOKA, D., 1984, *J. phys. Soc. Jpn.*, **53,** 3740.
[65] MELIK-ALAVERDIAN, V., BONESTEEL, N., and ORITZ, G., 1997, *Phys. Rev. Lett.*, **79,** 5286.
[66] MELIK-ALAVERDIAN, V., BONESTEEL, N., and ORITZ, G., 1997, *Physica* E, **1,** 138.
[67] HALDANE, F. D. M., 1985, *Phys. Rev. Lett.*, **55,** 2095.
[68] YOSHIOKA, D., 1986, *J. phys. Soc. Jpn.*, **55,** 3960.
[69] MAKSYM, P. A., 1985, *J. Phys.* C, **18,** L433.
[70] YOSHIOKA, D., 1986, *J. phys. Soc. Jpn.*, **55,** 885.
[71] FANG, F. F., and STILES P. J., 1968, *Phys. Rev.,* **174,** 823.
[72] CHAKRABORTY, T., and PIETILÄINEN, P., 1989, *Phys. Rev.* B, **39,** 7971.
[73] SYPHERS, D. A., and FURNEAUX, J. E., 1988, *Solid State Commun.*, **65,** 1513.
[74] MAAN, J. C., 1984, *Two-Dimensional Systems, Heterostructures and Superlattices*, edited by G. Bauer, F. Kucher and H. Heinrich (Heidelberg: Springer).
[75] BRUMMELL, M. A., HOPKINS, M. A., NICHOLAS, R. J., PORTAL, J. C., and CHENG, K. Y., 1986, *J. Phys.* C, **19,** L107.
[76] HALONEN, V., PIETILÄINEN, P., and CHAKRABORTY, T., 1990, *Phys. Rev.* B, **41,** 10 202.
[77] HAUG, R., KLITZING, K.v., NICHOLAS, R. J., MAAN, J. C., and WEIMANN, G., 1987, *Phys. Rev.* B, **36,** 4528.
[78] CLARK, R., and MAKSYM, P., 1989, *Phys. World,* **2,** 39.
[79] CLARK, R. G., HAYNES, S. R., SUCKLING, A. M., MALLETT, J. R., WRIGHT, P. A., HARRIS, J. J., and FOXON, C. T., 1989, *Phys. Rev. Lett.*, **62,** 1536.
[80] EISENSTEIN, J. P., STORMER, H. L., PFEIFFER, L., and WEST, K. W., 1989, *Phys. Rev. Lett.*, **62,** 1540.
[81] EISENSTEIN, J. P., STORMER, H. L., PFEIFFER, L., and WEST, K. W., 1989, *Phys. Rev.* B, **41,** 7910.
[82] CLARK, R. G., HAYNES, S. R., SUCKLING, A. M., MALLETT, J. R., WRIGHT, P. A., HARRIS, J. J., and FOXON, C. T., 1990, *Surf. Sci.*, **229,** 25.

[83] ENGEL, L., HWANG, S. W., SAJOTO, T., TSUI, D. C., and SHAYEGAN, M., 1992, *Phys. Rev.* B, **45,** 3418.
[84] SACHRAJDA, A., BOULET, R., WASILEWSKI, Z., and COLERIDGE, P., 1990, *Solid State Commun.*, **74,** 1021.
[85] BUCKTHOUGHT, A., BOULET, R., SACHRAJDA, A., WASILEWSKI, Z., ZAWADZKI, P., and GUILLON, F., 1991, *Solid State Commun.*, **78,** 191.
[86] FURNEAUX, J. E., SYPHERS, D. A., and SWANSON A. G., 1989, *Phys. Rev. Lett.*, **63,** 1098.
[87] KUKUSHKIN, I. V., VON KLITZING, K., and EBERL, K., 1997, *Phys. Rev.* B, **55,** 10607.
[88] KUKUSHKIN, I. V., VON KLITZING, K., and EBERL, K., 1997, *Physica* E, **1,** 21.
[89] DOROZHKIN, S. I., DOROKHOVA, M.O., HAUG, R. J., and PLOOG, K., 1997, *Phys. Rev.* B, **55,** 4089.
[90] DOROZHKIN, S. I., DOROKHOVA, M.O., HAUG, R. J., and PLOOG, K., 1997, *Physica* E, **1,** 59.
[91] BARRETT, S.E., DABBAGH, G., PFEIFFER, L. N., WEST, K. N., and TYCO, R., 1995, *Phys. Rev. Lett.*, **74,** 5112.
[92] BARRETT, S. E., TYCO, R., PFEIFFER, L. N., and WEST, K. N., 1994, *Phys. Rev. Lett.*, **72,** 1368.
[93] TYCO, R., BARRETT, S. E., DABBAGH, G., PFEIFFER, L. N., and WEST, K. N., 1995, *Science*, **268,** 1460.
[94] KHANDELWAL, P., KUZMA, N. N., BARRETT, S. E., PFEIFFER, L. N., and WEST, K. N., 1998, *Phys. Rev. Lett.*, **81,** 673.
[95] MANFRA, M. J., GOLDBERG, B. B., PFEIFFER, L. N., and WEST, K. N., 1996, *Phys. Rev.* B, **54,** R17327.
[96] MANFRA, M. J., GOLDBERG, B. B., PFEIFFER, L. N., and WEST, K. N., 1997, *Physica* E, **1,** 28.
[97] CHAKRABORTY, T., and PIETILÄINEN, P., 1996, *Phys. Rev. Lett.*, **76,** 4018.
[98] MORAWICZ, N. G., BARNHAM, K. W. J., BRIGGS, A., FOXON, C. T.,HARRIS, J. J., NAJDA, S.P., PORTAL, J. C., and WILLIAMS, M.L., 1993, *Semicond. Sci. Technol.*, **8,** 333.
[99] KANG, W., YOUNG, J. B., HANNAHS, S. T., PALM, E., CAMPMAN, K. L., and GOSSARD, A. C., 1997, *Phys. Rev.* B, **56,** R12776.
[100] LEADLEY, D. R., NICHOLAS, R. J., MAUDE, D. K., UTJUZH, A. N., PORTAL, J. C., HARRIS, J. J., and FOXON, C. T., 1997, *Phys. Rev. Lett.*, **79,** 4246.
[101] KRONMÜLLER, S., DIETSCHE, W., WEIS, J., VON KLITZING, K., WEGSCHEIDER, W., and BICHLER, M., 1998, *Phys. Rev. Lett.*, **81,** 2526.
[102] CHO, H., YOUNG, J. B., KANG, W., CAMPMAN, K. L., GOSSARD, A. C., BICHLER, M., and WEGSCHEIDER, W., 1998, *Phys. Rev. Lett.*, **81,** 2522.
[103] KRONMÜLLER, S., 1999, Dissertation, Max-Planck-Institute, Stuttgart, Germany.
[104] KRONMÜLLER, S., DIETSCHE, W., VON KLITZING, K., DENNINGER, G., WEGSCHEIDER, W., and BICHLER, M., 1999, *Phys. Rev. Lett.*, **82,** 4070.
[105] KUKUSHKIN, I. V., KLITZING, K. V., PLOOG, K., and TIMOFEEV, V. B., 1989, *Phys. Rev.* B, **40,** 7788.
[106] KUKUSHKIN, I. V., KLITZING, K. V., and EBERL, K., 1999, *Phys. Rev. Lett.*, **82,** 3665.
[107] NIEMELÄ, K., PIETILÄINEN, P., and CHAKRABORTY, T., 2000, *Physica* B, **284–288,** 1716.
[108] CHAKRABORTY, T., PIETILÄINEN, P., and SHANKAR, R., 1997, *Europhys. Lett.,* **38,** 141.
[109] READ, N., and SACHDEV, S., 1995, *Phys. Rev. Lett.*, **75,** 3509
[110] KASNER, M., and MACDONALD, A. H., 1995, *Physica* B, **212,** 289.
[111] KASNER, M., and MACDONALD, A. H., 1996, *Phys. Rev. Lett.*, **76,** 3204.
[112] SONG, Y.-Q., GOODSON, B. M., MARANOWSKI, K., and GOSSARD, A. C., 1999, *Phys. Rev. Lett.*, **82,** 2768.
[113] CHAKRABORTY, T., and PIETILÄINEN, P., 1999, *Phys. Rev. Lett.*, **83,** 5559.
[114] CHAKRABORTY, T., and PIETILÄINEN, P., 1988, *Phys. Rev.* B, **38,** 10 097.
[115] USHER, A., NICHOLAS, R. J., HARRIS, J. J., and FOXON, C. T., 1990, *Phys. Rev.* B, **41,** 1129.
[116] DOBERS, M., VON KLITZING, K., and WEIMANN, G., 1988, *Phys. Rev.* B, **38,** 5453.
[117] KALLIN, C., and HALPERIN, B. I., 1984, *Phys. Rev.* B, **30,** 5655.

[118] SONDHI, S. L., KARLHEDE, A., KIVELSON, S. A., and REZAYI, E., 1993, *Phys. Rev.* B, **47,** 16 419.
[119] FERTIG, H. A., BREY, L., COTE, R., and MACDONALD, A. H., 1994, *Phys. Rev.* B, **50,** 11018.
[120] KRALIK, B., RAPPE, A. M., and LOUIE, S. G., 1995, *Phys. Rev.* B, **52,** R11 616.
[121] KRALIK, B., RAPPE, A. M., and LOUIE, S. G., 1997, *Phys. Rev.* B, **56,** 4760.
[122] AIFER, E. H., GOLDBERG, B. B., and BROIDO, D. A., 1995, *Phys. Rev. Lett.*, **76,** 680.
[123] SCHMELLER, A., EISENSTEIN, J. P., PFEIFFER, L. N., and WEST, K. N., 1995, *Phys. Rev. Lett.*, **75,** 4290.
[124] MAUDE, D. K., POTEMSKI, M., HENINI, M., EAVES, L., HILL, G., and PATE, M. A., 1996, *Phys. Rev. Lett.*, **77,** 4604.
[125] JAIN, J. K., and WU, X. G., 1994, *Phys. Rev.* B, **49,** 5085.
[126] WU, X. G., and SONDHI, S. L., 1995, *Phys. Rev.* B, **51,** 14 725.
[127] COOPER, N. R., 1997, *Phys. Rev.* B, **55,** R1934.
[128] BAYOT, V., GRIVEI, E., MELINTE, S., SANTOS, M. B., and SHAYEGAN, M., 1996, *Phys. Rev. Lett.,* **76,** 4584.
[129] BAYOT, V., GRIVEI, E., BEUKEN, J.-M., MELINTE, S., and SHAYEGAN, M., 1997, *Phys. Rev. Lett.,* **79,** 1718.
[130] COTE, R., MACDONALD, A. H., BREY, L., FERTIG, H. A., GIRVIN, S. M., and STOOF, H. T. C., 1997, *Phys. Rev. Lett.*, **78,** 4825.
[131] MELINTE, S., GRIVEI, E., BAYOT, V., and SHAYEGAN, 1999, *Phys. Rev. Lett.*, **82,** 2764.
[132] DOLGOPOLOV, V. T., SHASHKIN, A. A., ARISTOV, A. V., SCHMEREK, D., HANSEN, W., KOTTHAUS, J. P., and HOLLAND, M., 1997, *Phys. Rev. Lett.*, **79,** 729.
[133] PINCZUK, A., 1992, *Festkörperprobleme/Advances in Solid State Physics*, **32,** 45.
[134] CHAKRABORTY, T., and PIETILÄINEN, P., 1987, *Phys. Rev. Lett.*, **59,** 2784.
[135] EISENSTEIN, J. P., BOEBINGER, G. S., PFEIFFER, L. N., WEST, K. W., and HE, S., 1992, *Phys. Rev. Lett.*, **68,** 1383.
[136] PELLEGRINI, V., PINCZUK, A., DENNIS, B. S., PLAUT, A. S., PFEIFFER, L. N., and WEST, K. W., 1997, *Phys. Rev. Lett.*, **78,** 310.
[137] SAWADA, A., EZAWA, Z. F., OHNO, H., HORIKOSHI, Y., OHNO, Y., KISHIMOTO, S., MATSUKURA, F., YASUMOTO, M., and URAYAMA, A., 1998, *Phys. Rev. Lett.*, **80,** 4534.
[138] CHAKRABORTY, T., NIEMELA, K., and PIETILÄINEN, P., 1997, *Phys. Rev. Lett.*, **78,** 4829; 1998, *Phys. Rev.* B, **58,** 9890; 1999, *Physica* E, **1,** 80.
[139] CHAKRABORTY, T., 1999, *Festkörperprobleme/Advances in Solid State Physics*, Vol. 38, p. 397.
[140] TIMP, G., BEHRINGER, R., CUNNINGHAM, J. E., and HOWARD, R. E., 1989, *Phys. Rev. Lett.*, **63,** 2268; Timp, G., 1992, *Nanostructured Systems*, edited by M. Reed (Boston, MA: Academic), Ch. 3.
[141] YOSHIOKA, D., 1993, *Physica* B, **184,** 86; 1993, *J. phys. Soc. Jpn.*, **62,** 839; Tokizaki, S., and KURAMOTO. Y., 1995, *J. phys. Soc. Jpn.*, **64,** 2302.
[142] HALPERIN, B. I., 1997, *Perspectives in Quantum Hall Effects*, edited by S. Das Sarma and A. Pinczuk (New York: Wiley).
[143] SIMON, S. H., 1999, *Composite Fermions,* edited by O. Heinonen (Singapore: World Scientific).
[144] DU, R. R., YEH, A. S., STORMER, H. L., TSUI, D. C., PFEIFFER, L. N., and WEST, K. W., 1995, *Phys. Rev. Lett.*, **75,** 3926.
[145] STÖRMER, H. L., and TSUI, D. C., 1997, *Perspectives in Quantum Hall Effects*, edited by S. Das Sarma and A. Pinczuk (New York: Wiley).
[146] JIANG, H. W., STORMER, H. L., TSUI, D. C., PFEIFFER, L. N., and WEST, K. W., 1989, *Phys. Rev.* B, **40,** 12 013.
[147] NIEMELÄ, K., PIETILÄINEN, P., and CHAKRABORTY, T., Cond-mat/0007043.
[148] APALKOV, V., CHAKRABORTY, T., PIETILÄINEN, P., and NIEMELÄ, K., Cond-mat/0007168.
[149] EISENSTEIN, J. P., WILLETT, R. L., STORMER, H. L., PFEIFFER, L. N., and WEST, K. W., 1990, *Surf. Sci.*, **229,** 31.
[150] HALDANE, F. D. M., and REZAYI, E. H., 1988, *Phys. Rev. Lett.*, **60,** 956.
[151] MACDONALD, A. H., YOSHIOKA, D., and GIRVIN, S. M., 1989, *Phys. Rev.* B, **39,** 8044.